

QCD Sum Rules Analysis of Weak Decays of Doubly-Heavy Baryons

Yu-Ji Shi¹ *, Wei Wang¹ †, and Zhen-Xing Zhao¹ ‡

¹ *INPAC, SKLPPC, School of Physics and Astronomy,
Shanghai Jiao Tong University, Shanghai 200240, China*

We calculate the weak decay form factors of doubly-heavy baryons using three-point QCD sum rules. The Cutkosky rules are used to derive the double dispersion relations. We include perturbative contributions and condensation contributions up to dimension five, and point out that the perturbative contributions and condensates with lowest dimensions dominate. An estimate of part of gluon-gluon condensates show that it plays a less important role. With these form factors at hand, we present a phenomenological study of semileptonic decays. The future experimental facilities can test these predictions, and deepen our understanding of the dynamics in decays of doubly-heavy baryons.

I. INTRODUCTION

Although quark model has achieved many brilliant successes in hadron spectroscopy, not all predicted particles, even in ground-state, in the quark model have been experimentally established so far. These states include doubly-heavy baryons and triply-heavy baryons. In 2017, the LHCb collaboration has reported the first observation of doubly-charmed baryon Ξ_{cc}^{++} with the mass [1]

$$m_{\Xi_{cc}^{++}} = (3621.40 \pm 0.72 \pm 0.27 \pm 0.14) \text{ MeV} \quad (1)$$

in the $\Lambda_c^+ K^- \pi^+ \pi^+$ final state. Soon afterwards new results on Ξ_{cc}^{++} were released by LHCb, including the first measurement of its lifetime [2] and the observation of a new decay mode $\Xi_{cc}^{++} \rightarrow \Xi_c^+ \pi^+$ [3]. On experimental side, more investigations on Ξ_{cc}^{++} and searches for other doubly-heavy baryons are certainly demanded to achieve a better understanding [4, 5]. Meanwhile these observations have triggered many theoretical studies on various properties of doubly-heavy baryons [5–42], most of which have been focused on the spectrum, production and decay properties.

In a previous work [6], we have performed an analysis of decay form factors of doubly-heavy baryons in a light-front quark model (LFQM). In this light-front study, the diquark picture is adopted, where the two spectator quarks are treated as a bounded system. This approximation can greatly simplify the calculation and many useful phenomenological results are obtained [28, 33]. But meanwhile this diquark approximation introduces uncontrollable systematic uncertainties since the dynamics in the diquark system has been smeared. In this work, we will remedy this shortcoming and perform an analysis of transition form factors using QCD sum rules (QCDSR). Some earlier

* Corresponding author, Email: shiyuji@sjtu.edu.cn

† Corresponding author, Email: wei.wang@sjtu.edu.cn

‡ Corresponding author, Email: star_0027@sjtu.edu.cn

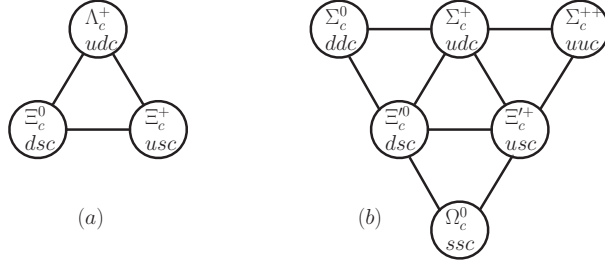


FIG. 1: The anti-triplet (panel a) and sextet (panel b) of charmed baryons. It is similar for bottom baryons.

attempts basing on non-relativistic QCD (NRQCD) sum rules can be found in Refs. [43–45]. It is necessary to note that since the decay final state contains only one heavy quark, NRQCD should not be applicable unless the strange quark is also treated as a heavy quark. In the literature the QCDSR framework has also been used to calculate masses and the pole residues of doubly heavy baryons in a number of references (see for instance [18, 46–49]). So it is desirable to calculate the decay form factors within the same framework, which is the motif of this work.

In our analysis, the doubly heavy baryons include $\Xi_{cc}(ccq)$, $\Omega_{cc}(ccs)$, $\Xi_{bb}(bbq)$, $\Omega_{bb}(bbs)$, and $\Xi_{bc}(bcq)$, $\Omega_{bc}(bcs)$, with $q = u, d$. The $\Xi_{QQ'}$ and $\Omega_{QQ'}$ can form a flavor SU(3) triplet. It should be noted that the two heavy quarks in Ξ_{bc} and Ω_{bc} are symmetric in the flavor space. The antisymmetric case that presumably will decay via strong or electromagnetic interactions are not considered in this work. Quantum numbers of doubly heavy baryons can be found in Table I. Baryons in the final state contains one heavy bottom/charm quark and two light quarks. They can form an SU(3) anti-triplet Λ_Q , Ξ_Q or an SU(3) sextet Σ_Q , Ξ'_Q and Ω_Q with $Q = b, c$, as depicted in Fig. 1.

TABLE I: Quantum numbers and quark content for the lowest-lying doubly heavy baryons. S_h^π denotes the spin/parity of the system of two heavy quarks. The light quark q corresponds to the u, d quark.

Baryon	Quark content	S_h^π	J^P	Baryon	Quark content	S_h^π	J^P
Ξ_{cc}	$\{cc\}q$	1^+	$1/2^+$	Ξ_{bb}	$\{bb\}q$	1^+	$1/2^+$
Ξ_{cc}^*	$\{cc\}q$	1^+	$3/2^+$	Ξ_{bb}^*	$\{bb\}q$	1^+	$3/2^+$
Ω_{cc}	$\{cc\}s$	1^+	$1/2^+$	Ω_{bb}	$\{bb\}s$	1^+	$1/2^+$
Ω_{cc}^*	$\{cc\}s$	1^+	$3/2^+$	Ω_{bb}^*	$\{bb\}s$	1^+	$3/2^+$
Ξ'_{bc}	$[bc]q$	0^+	$1/2^+$	Ω'_{bc}	$[bc]s$	0^+	$1/2^+$
Ξ_{bc}	$\{bc\}q$	1^+	$1/2^+$	Ω_{bc}	$\{bc\}s$	1^+	$1/2^+$
Ξ_{bc}^*	$\{bc\}q$	1^+	$3/2^+$	Ω_{bc}^*	$\{bc\}s$	1^+	$3/2^+$

To be more explicit, the transitions of doubly heavy baryons can be classified as follows:

- The cc sector

$$\Xi_{cc} \rightarrow [\Lambda_c, \Xi_c, \Sigma_c, \Xi'_c], \quad \Omega_{cc} \rightarrow [\Xi_c, \Xi'_c],$$

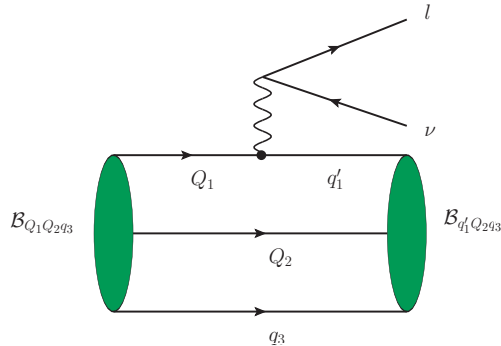


FIG. 2: Feynman diagram for semileptonic decays. The leptonic amplitude can be calculated using perturbation theory, while hadronic matrix elements can be parametrized into form factors.

- The bb sector

$$\Xi_{bb} \rightarrow [\Lambda_b, \Sigma_b], \quad \Omega_{bb} \rightarrow [\Xi_b, \Xi'_b],$$

- The bc sector with c quark decay

$$\Xi_{bc} \rightarrow [\Lambda_b, \Xi_b, \Sigma_b, \Xi'_b], \quad \Omega_{bc} \rightarrow [\Xi_b, \Xi'_b],$$

- The bc sector with b quark decay

$$\Xi_{bc} \rightarrow [\Lambda_c, \Sigma_c], \quad \Omega_{bc} \rightarrow [\Xi_c, \Xi'_c].$$

In the above, both SU(3) anti-triplet and sextet final states are taken into account. However, the $b \rightarrow c$ transition will not be considered in this work, and is left for future.

The rest of this paper is arranged as follows. In Sec. II, the transition form factors are calculated in QCDSR, where the perturbative contribution, quark condensates, quark-gluon condensates are calculated and an estimate of part of gluon-gluon condensates is presented. Numerical results for form factors are presented in Sec. III, which are subsequently used to perform the phenomenological studies in Sec. IV. A brief summary of this work and the prospect for the future are given in the last section.

II. TRANSITION FORM FACTORS IN QCD SUM RULES

A. Form Factors

We show the Feynman diagram for semileptonic decays of doubly-heavy baryons in Fig. 2. The leptonic amplitude in this transition can be calculated using electro-weak perturbation theory, while the hadronic matrix elements can be parametrized into transition form factors:

$$\langle \mathcal{B}_2(p_2) | (V - A)_\mu | \mathcal{B}_1(p_1) \rangle = \bar{u}(p_2, s_2) \left[\gamma_\mu f_1(q^2) + i\sigma_{\mu\nu} \frac{q^\nu}{M_1} f_2(q^2) + \frac{q_\mu}{M_1} f_3(q^2) \right] u(p_1, s_1)$$

$$-\bar{u}(p_2, s_2) \left[\gamma_\mu g_1(q^2) + i\sigma_{\mu\nu} \frac{q^\nu}{M_1} g_2(q^2) + \frac{q_\mu}{M_1} g_3(q^2) \right] \gamma_5 u(p_1, s_1), \quad (2)$$

where $p_1(s_1)$ is the momentum (spin) of the initial state, and $p_2(s_2)$ is the momentum (spin) of the final baryon. The momentum transfer is defined as $q^\mu = p_1^\mu - p_2^\mu$, and the vector (axial-vector) $V^\mu (A^\mu)$ is defined as $\bar{q}'_1 \gamma^\mu (\gamma^\mu \gamma^5) Q_1$, with q'_1 being a light quark and Q_1 as a heavy bottom or charm quark. M_1 is the mass of the initial doubly-heavy baryon. These form factors are also responsible for non-leptonic decay modes if the factorization holds, and thus must be calculated in a nonperturbative manner for later use.

In our calculation, the following simple parametrization will be used first:

$$\begin{aligned} \langle \mathcal{B}_2(p_2, s_2) | (V - A)_\mu | \mathcal{B}_1(p_1, s_1) \rangle &= \bar{u}(p_2, s_2) \left[\frac{p_1^\mu}{M_1} F_1 + \frac{p_2^\mu}{M_2} F_2 + \gamma_\mu F_3 \right] u(p_1, s_1) \\ &- \bar{u}(p_2, s_2) \left[\frac{p_1^\mu}{M_1} G_1 + \frac{p_2^\mu}{M_2} G_2 + \gamma_\mu G_3 \right] \gamma_5 u(p_1, s_1). \end{aligned} \quad (3)$$

Once the form factors F_i and G_i in Eq. (3) are obtained, then they will be transformed into f_i and g_i in Eq. (2), which are used to compared with other works in the literature.

B. QCD Sum Rules

The starting point in QCDSR is to construct a suitable correlation function, and for the $\mathcal{B}_{Q_1 Q_2 q_3} \rightarrow \mathcal{B}_{q'_1 Q_2 q_3}$ transition, it is chosen as:

$$\Pi_\mu^{V,A}(p_1^2, p_2^2, q^2) = i^2 \int d^4x d^4y e^{-ip_1 \cdot x + ip_2 \cdot y} \langle 0 | T \{ J_{\mathcal{B}_{q'_1 Q_2 q_3}}(y) (V_\mu, A_\mu)(0) \bar{J}_{\mathcal{B}_{Q_1 Q_2 q_3}}(x) \} | 0 \rangle. \quad (4)$$

Here the weak transition $Q_1 \rightarrow q'_1$ stands for the $c \rightarrow d/s$ or $b \rightarrow u$ process. The $Q_2 = c/b$, $q_3 = u/d/s$ and $V_\mu (A_\mu) = \bar{q}'_1 \gamma_\mu (\gamma_\mu \gamma_5) Q_1$. The $J_{\mathcal{B}_{q'_1 Q_2 q_3}}$ and $J_{\mathcal{B}_{Q_1 Q_2 q_3}}$ are the interpolating currents for singly and doubly heavy baryons respectively. For Ξ_{QQ} and Ω_{QQ} , they are used as:

$$\begin{aligned} J_{\Xi_{QQ}} &= \epsilon_{abc} (Q_a^T C \gamma^\mu Q_b) \gamma_\mu \gamma_5 q_c, \\ J_{\Omega_{QQ}} &= \epsilon_{abc} (Q_a^T C \gamma^\mu Q_b) \gamma_\mu \gamma_5 s_c, \end{aligned} \quad (5)$$

where $Q = b, c$ and $q = u, d$. For Ξ_{bc} and Ω_{bc} the interpolating currents are

$$\begin{aligned} J_{\Xi_{bc}} &= \frac{1}{\sqrt{2}} \epsilon_{abc} (b_a^T C \gamma^\mu c_b + c_a^T C \gamma^\mu b_b) \gamma_\mu \gamma_5 q_c, \\ J_{\Omega_{bc}} &= \frac{1}{\sqrt{2}} \epsilon_{abc} (b_a^T C \gamma^\mu c_b + c_a^T C \gamma^\mu b_b) \gamma_\mu \gamma_5 s_c, \end{aligned} \quad (6)$$

where b and c fields are chosen symmetric. The interpolating currents for singly heavy baryons can be defined in a similar way. For the SU(3) anti-triplet they are

$$J_{\Lambda_Q} = \frac{1}{\sqrt{2}} \epsilon_{abc} (u_a^T C \gamma_5 d_b - d_a^T C \gamma_5 u_b) Q_c,$$

$$J_{\Xi_Q} = \frac{1}{\sqrt{2}}\epsilon_{abc}(q_a^T C \gamma_5 s_b - s_a^T C \gamma_5 q_b) Q_c, \quad (7)$$

and for the SU(3) sextet they are

$$\begin{aligned} J_{\Sigma_Q} &= \frac{1}{\sqrt{2}}\epsilon_{abc}(u_a^T C \gamma^\mu d_b + d_a^T C \gamma^\mu u_b)\gamma_\mu \gamma_5 Q_c, \\ J_{\Xi'_Q} &= \frac{1}{\sqrt{2}}\epsilon_{abc}(q_a^T C \gamma^\mu s_b + s_a^T C \gamma^\mu q_b)\gamma_\mu \gamma_5 Q_c, \\ J_{\Omega_Q} &= \epsilon_{abc}s_a^T C \gamma^\mu s_b \gamma_\mu \gamma_5 Q_c. \end{aligned} \quad (8)$$

Similar definitions for the interpolating currents were adopted in Refs. [46, 47, 54], and some discussions can be found in Ref. [46].

The correlation function can be calculated at both hadron and QCD level. In the following, we will only present the extraction of the vector-current form factors, and the axial-vector-current form factors can be determined in a similar way. At hadron level, one can insert complete sets of the initial and final hadronic states into the correlation function and consider the contributions from positive and negative parity baryons simultaneously, then the correlation function can be written as

$$\begin{aligned} \Pi_\mu^{V,\text{had}} &= \lambda_f^+ \lambda_i^+ \frac{(\not{p}_2 + M_2^+)(\frac{p_{1\mu}}{M_1^+} F_1^{++} + \frac{p_{2\mu}}{M_2^+} F_2^{++} + \gamma_\mu F_3^{++})(\not{p}_1 + M_1^+)}{(p_2^2 - M_2^{+2})(p_1^2 - M_1^{+2})} \\ &+ \lambda_f^+ \lambda_i^- \frac{(\not{p}_2 + M_2^+)(\frac{p_{1\mu}}{M_1^-} F_1^{+-} + \frac{p_{2\mu}}{M_2^+} F_2^{+-} + \gamma_\mu F_3^{+-})(\not{p}_1 - M_1^-)}{(p_2^2 - M_2^{+2})(p_1^2 - M_1^{-2})} \\ &+ \lambda_f^- \lambda_i^+ \frac{(\not{p}_2 - M_2^-)(\frac{p_{1\mu}}{M_1^+} F_1^{-+} + \frac{p_{2\mu}}{M_2^-} F_2^{-+} + \gamma_\mu F_3^{-+})(\not{p}_1 + M_1^+)}{(p_2^2 - M_2^{-2})(p_1^2 - M_1^{+2})} \\ &+ \lambda_f^- \lambda_i^- \frac{(\not{p}_2 - M_2^-)(\frac{p_{1\mu}}{M_1^-} F_1^{--} + \frac{p_{2\mu}}{M_2^-} F_2^{--} + \gamma_\mu F_3^{--})(\not{p}_1 - M_1^-)}{(p_2^2 - M_2^{-2})(p_1^2 - M_1^{-2})} \\ &+ \dots \end{aligned} \quad (9)$$

In Eq. (9), the ellipsis stands for the contribution from higher resonances and continuum spectra, $M_{1(2)}^{+(-)}$ denotes the mass of the initial (final) positive (negative) parity baryons, and F_1^{-+} is the form factor F_1 defined in Eq. (3) with the negative-parity final state and the positive-parity initial state, and so forth. To arrive at Eq. (9), we have adopted the pole residue definitions for positive and negative parity baryons

$$\begin{aligned} \langle 0 | J_+ | \mathcal{B}_+(p, s) \rangle &= \lambda_+ u(p, s), \\ \langle 0 | J_+ | \mathcal{B}_-(p, s) \rangle &= (i\gamma_5) \lambda_- u(p, s), \end{aligned} \quad (10)$$

and the following conventions for the form factors $F_i^{\pm\pm}$:

$$\langle \mathcal{B}_f^+(p_2, s_2) | V_\mu | \mathcal{B}_i^+(p_1, s_1) \rangle = \bar{u}(p_2, s_2) \left[\frac{p_{1\mu}}{M_1^+} F_1^{++} + \frac{p_{2\mu}}{M_2^+} F_2^{++} + \gamma_\mu F_3^{++} \right] u(p_1, s_1),$$

$$\begin{aligned}
\langle \mathcal{B}_f^+(p_2, s_2) | V_\mu | \mathcal{B}_i^-(p_1, s_1) \rangle &= \bar{u}(p_2, s_2) \left[\frac{p_{1\mu}}{M_1^-} F_1^{+-} + \frac{p_{2\mu}}{M_2^+} F_2^{+-} + \gamma_\mu F_3^{+-} \right] (i\gamma_5) u(p_1, s_1), \\
\langle \mathcal{B}_f^-(p_2, s_2) | V_\mu | \mathcal{B}_i^+(p_1, s_1) \rangle &= \bar{u}(p_2, s_2) (i\gamma_5) \left[\frac{p_{1\mu}}{M_1^+} F_1^{-+} + \frac{p_{2\mu}}{M_2^-} F_2^{-+} + \gamma_\mu F_3^{-+} \right] u(p_1, s_1), \\
\langle \mathcal{B}_f^-(p_2, s_2) | V_\mu | \mathcal{B}_i^-(p_1, s_1) \rangle &= \bar{u}(p_2, s_2) (i\gamma_5) \left[\frac{p_{1\mu}}{M_1^-} F_1^{--} + \frac{p_{2\mu}}{M_2^-} F_2^{--} + \gamma_\mu F_3^{--} \right] (i\gamma_5) u(p_1, s_1). \quad (11)
\end{aligned}$$

In Eq. (10), J_+ can be found in Eqs. (5-8), and $\lambda_{+(-)}$ is the pole residue for the positive (negative) parity baryon.

At the QCD level, the correlation function can be evaluated using the operator product expansion (OPE), and expanded as a power of matrix elements of local operators in the deep Euclidean momentum region. This expansion is organized by the inverse of mass dimensions. The identity operator corresponds to the so-called perturbative term and higher dimensional operators are called the condensate terms. A detailed calculation of these contributions will be presented in the following subsections, including the perturbative contribution (dim-0), the quark condensate contribution (dim-3) and the mixed quark-gluon condensate contribution (dim-5). For practical use, it is convenient to express the correlation function as a double dispersion relation

$$\Pi_\mu^{V,\text{QCD}}(p_1^2, p_2^2, q^2) = \int^\infty ds_1 \int^\infty ds_2 \frac{\rho_\mu^{V,\text{QCD}}(s_1, s_2, q^2)}{(s_1 - p_1^2)(s_2 - p_2^2)}, \quad (12)$$

with $\rho_\mu^{V,\text{QCD}}(s_1, s_2, q^2)$ being the spectral function, which can be obtained by applying Cutkosky cutting rules. Quark-hadron duality guarantees that results for correlation functions derived at hadron level and QCD level are equivalent. In particular, it is plausible to identify the spectral functions above threshold at the hadron level and QCD level. Under this assumption, the sum of the four pole terms in Eq. (9) should be equal to

$$\int^{s_1^0} ds_1 \int^{s_2^0} ds_2 \frac{\rho_\mu^{V,\text{QCD}}(s_1, s_2, q^2)}{(s_1 - p_1^2)(s_2 - p_2^2)} \equiv \Pi_\mu^{V,\text{pole}}, \quad (13)$$

where $s_{1(2)}^0$ is the threshold parameter for the initial (final) baryon. $\Pi_\mu^{V,\text{pole}}$ can be formally written as

$$\Pi_\mu^{V,\text{pole}} = \sum_{i=1}^{12} A_i e_{i\mu}, \quad (14)$$

where, for latter convenience, we define

$$\begin{aligned}
(e_{1,2,3,4})_\mu &= \{\not{p}_2, 1\} \times \{p_{1\mu}\} \times \{\not{p}_1, 1\}, \\
(e_{5,6,7,8})_\mu &= \{\not{p}_2, 1\} \times \{p_{2\mu}\} \times \{\not{p}_1, 1\}, \\
(e_{9,10,11,12})_\mu &= \{\not{p}_2, 1\} \times \{\gamma_\mu\} \times \{\not{p}_1, 1\}. \quad (15)
\end{aligned}$$

Then one can obtain these 12 form factors $F_i^{\pm,\pm}$ in Eq. (9) by comparing the corresponding coefficients of these 12 Dirac structures at hadronic and QCD levels. Especially, one can obtain the expressions for F_i^{++} as:

$$\begin{aligned}
\frac{\lambda_i^+ \lambda_f^+(F_1^{++}/M_1^+)}{(p_1^2 - M_1^{+2})(p_2^2 - M_2^{+2})} &= \frac{\{M_1^- M_2^-, M_2^-, M_1^-, 1\} \cdot \{A_1, A_2, A_3, A_4\}}{(M_1^+ + M_1^-)(M_2^+ + M_2^-)}, \\
\frac{\lambda_i^+ \lambda_f^+(F_2^{++}/M_2^+)}{(p_1^2 - M_1^{+2})(p_2^2 - M_2^{+2})} &= \frac{\{M_1^- M_2^-, M_2^-, M_1^-, 1\} \cdot \{A_5, A_6, A_7, A_8\}}{(M_1^+ + M_1^-)(M_2^+ + M_2^-)}, \\
\frac{\lambda_i^+ \lambda_f^+ F_3^{++}}{(p_1^2 - M_1^{+2})(p_2^2 - M_2^{+2})} &= \frac{\{M_1^- M_2^-, M_2^-, M_1^-, 1\} \cdot \{A_9, A_{10}, A_{11}, A_{12}\}}{(M_1^+ + M_1^-)(M_2^+ + M_2^-)}. \tag{16}
\end{aligned}$$

In practice Borel transformation are usually adopted to improve the convergence in the quark-hadron duality and suppress the higher resonance and continuum contributions:

$$\begin{aligned}
\lambda_i^+ \lambda_f^+(F_1^{++}/M_1^+) \exp\left(-\frac{M_1^{+2}}{T_1^2} - \frac{M_2^{+2}}{T_2^2}\right) &= \frac{\{M_1^- M_2^-, M_2^-, M_1^-, 1\} \cdot \{\mathcal{B}A_1, \mathcal{B}A_2, \mathcal{B}A_3, \mathcal{B}A_4\}}{(M_1^+ + M_1^-)(M_2^+ + M_2^-)}, \\
\lambda_i^+ \lambda_f^+(F_2^{++}/M_2^+) \exp\left(-\frac{M_1^{+2}}{T_1^2} - \frac{M_2^{+2}}{T_2^2}\right) &= \frac{\{M_1^- M_2^-, M_2^-, M_1^-, 1\} \cdot \{\mathcal{B}A_5, \mathcal{B}A_6, \mathcal{B}A_7, \mathcal{B}A_8\}}{(M_1^+ + M_1^-)(M_2^+ + M_2^-)}, \\
\lambda_i^+ \lambda_f^+ F_3^{++} \exp\left(-\frac{M_1^{+2}}{T_1^2} - \frac{M_2^{+2}}{T_2^2}\right) &= \frac{\{M_1^- M_2^-, M_2^-, M_1^-, 1\} \cdot \{\mathcal{B}A_9, \mathcal{B}A_{10}, \mathcal{B}A_{11}, \mathcal{B}A_{12}\}}{(M_1^+ + M_1^-)(M_2^+ + M_2^-)}, \tag{17}
\end{aligned}$$

where $\mathcal{B}A_i \equiv \mathcal{B}_{T_1^2, T_2^2} A_i$ are doubly Borel transformed coefficients, and T_1^2 and T_2^2 are the Borel mass parameters.

The coefficients A_i in Eq. (14) can be projected out in the following way. Multiplying by e_j^μ then taking the trace on the both sides of Eq. (14), one can arrive at the following 12 linear equations:

$$B_j \equiv \text{Tr}[\Pi_\mu^{V, \text{pole}} e_j^\mu] = \text{Tr} \left[\left(\sum_{i=1}^{12} A_i e_{i\mu} \right) e_j^\mu \right], \quad j = 1, \dots, 12, \tag{18}$$

Solving these equations one can obtain these A_i .

In the following, we will use the vector-current form factors for doubly-heavy baryon into a SU(3) sextet baryon as an example to illustrate our calculation. Results for other transitions can be obtained in a similar manner.

C. The perturbative contribution

The perturbative contribution is derived by computing the coefficient of the identity operator in OPE. The corresponding Feynman diagram is shown in Fig. 3. The doubly-solid line denotes a heavy bottom/charm quark, and the ordinary solid line corresponds to a light quark. Its contribution is given as

$$\Pi_\mu^{V, \text{pert}}(p_1^2, p_2^2, q^2) = 6 \cdot 2\sqrt{2} i^2 \int \frac{d^4 k_2}{(2\pi)^4} \frac{d^4 k_3}{(2\pi)^4} \frac{N_\mu}{(k_1^2 - m_1^2)(k_1'^2 - m_1'^2)(k_2^2 - m_2^2)(k_3^2 - m_3^2)}, \tag{19}$$

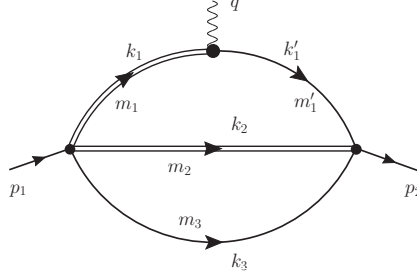


FIG. 3: The perturbative contribution to transition form factors. The doubly-solid line denotes a heavy quark, and the ordinary solid line corresponds to a light quark.

where the factor 6 comes from the color contraction $\epsilon_{abc}\epsilon^{abc}$, the factor $2\sqrt{2}$ comes from the contraction of quark fields and the normalization factors of the baryon currents. The numerator of the integrand in Eq. (19) is:

$$\begin{aligned} N_\mu &= \gamma_{\alpha'}\gamma_5(\not{k}_2 + m_2)\gamma^\alpha(\not{k}_1 - m_1)\gamma_\mu(\not{k}'_1 - m'_1)\gamma^{\alpha'}(\not{k}_3 + m_3)\gamma_\alpha\gamma_5, \\ k_1 &= p_1 - k_2 - k_3, \quad k'_1 = p_2 - k_2 - k_3. \end{aligned} \quad (20)$$

The correlation function can be expressed in terms of a double dispersion integration:

$$\Pi_\mu^{V,\text{pert}}(p_1^2, p_2^2, q^2) = \int ds_1 ds_2 \frac{\rho_\mu^{V,\text{pert}}(s_1, s_2, q^2)}{(s_1 - p_1^2)(s_2 - p_2^2)}. \quad (21)$$

Here the spectral function $\rho_\mu^{V,\text{pert}}(s_1, s_2, q^2)$ is proportional to the discontinuity of the correlation function with respect to s_1 and s_2 . According to the Cutkosky rule, the spectral function can be obtained by setting all the propagators onshell:

$$\rho_\mu^{V,\text{pert}}(s_1, s_2, q^2) = \frac{(-2\pi i)^4}{(2\pi i)^2} (12\sqrt{2}i^2) \int \frac{d^4 k_2}{(2\pi)^4} \frac{d^4 k_3}{(2\pi)^4} \delta(k_1^2 - m_1^2) \delta(k_1'^2 - m_1'^2) \delta(k_2^2 - m_2^2) \delta(k_3^2 - m_3^2) N_\mu. \quad (22)$$

The phase-space-like integral can be evaluated as:

$$\int d^4 k_2 d^4 k_3 \delta(k_1^2 - m_1^2) \delta(k_1'^2 - m_1'^2) \delta(k_2^2 - m_2^2) \delta(k_3^2 - m_3^2) = \int dm_{23}^2 \int_{\Delta} \int_2, \quad (23)$$

where

$$\begin{aligned} \int_{\Delta} &\equiv \int d^4 k_1 d^4 k'_1 d^4 k_{23} \delta(k_1^2 - m_1^2) \delta(k_1'^2 - m_1'^2) \delta(k_{23}^2 - m_{23}^2) \delta^4(p_1 - k_1 - k_{23}) \delta^4(p_2 - k'_1 - k_{23}), \\ \int_2 &\equiv \int d^4 k_2 d^4 k_3 \delta(k_2^2 - m_2^2) \delta(k_3^2 - m_3^2) \delta^4(k_{23} - k_2 - k_3). \end{aligned} \quad (24)$$

D. The quark condensate contribution

The $\bar{q}q$ condensate operator in the OPE has dimension 3, and its Feynman diagram is shown in Fig. 4. Since heavy quarks will not contribute with condensations, there are two diagrams from

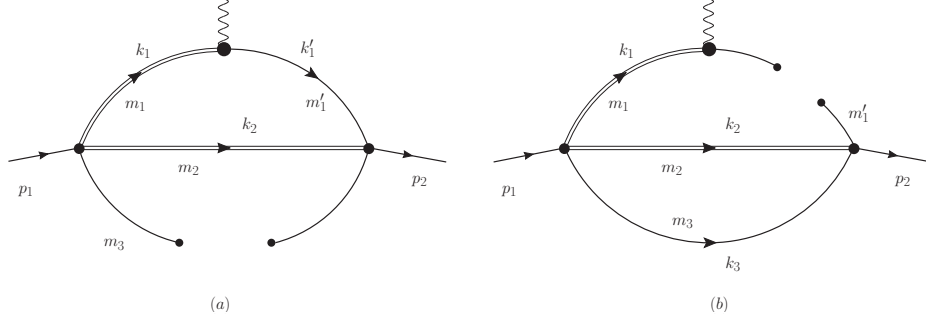


FIG. 4: Light-quark condensate diagrams. Heavy quark will not condensate and thus only the two light-quark propagators give condensate contributions.

the light quark condensate. The diagram (4a) gives:

$$\Pi_{\mu}^{V, \langle \bar{q}q \rangle, a}(p_1^2, p_2^2, q^2) = (-6 \cdot 2\sqrt{2}i) \frac{1}{12} \langle \bar{q}q \rangle \int \frac{d^4 k_2}{(2\pi)^4} \frac{N_{\mu}^{V, \langle \bar{q}q \rangle, a}}{(k_1^2 - m_1^2)(k_1'^2 - m_1'^2)(k_2^2 - m_2^2)}, \quad (25)$$

where the condensate term is defined as $\langle q_a^i \bar{q}_b^j \rangle = -(\langle \bar{q}q \rangle / 12) \delta_{ab} \delta^{ij}$, and the numerator is:

$$\begin{aligned} N_{\mu}^{V, \langle \bar{q}q \rangle, a} &= \gamma_{\alpha'} \gamma_5 (\not{k}_2 + m_2) \gamma^{\alpha} (\not{k}_1 - m_1) \gamma_{\mu} (\not{k}_1' - m_1') \gamma^{\alpha'} \gamma_{\alpha} \gamma_5, \\ k_1 &= p_1 - k_2, \quad k_1' = p_2 - k_2. \end{aligned} \quad (26)$$

According to the Cutkosky rule, the spectral function can now be evaluated as:

$$\rho_{\mu}^{V, \langle \bar{q}q \rangle, a}(s_1, s_2, q^2) = \frac{1}{(2\pi i)^2} (-2\pi i)^3 (-\sqrt{2}i) \langle \bar{q}q \rangle \frac{1}{(2\pi)^4} \int_{\Delta} N_{\mu}^{V, \langle \bar{q}q \rangle, a}, \quad (27)$$

where the integral \int_{Δ} is slightly different from that in Eq. (24), with m_{23}^2 being replaced by m_2^2 . The diagram (b) has the amplitude:

$$\Pi_{\mu}^{V, \langle \bar{q}q \rangle, b}(p_1^2, p_2^2, q^2) \sim \int \frac{d^4 k_2}{(2\pi)^4} \frac{N_{\mu}^{V, \langle \bar{q}q \rangle, b}}{(q^2 - m_1^2)(k_2^2 - m_2^2)((p_2 - k_2)^2 - m_3^2)}. \quad (28)$$

One can see that the denominator is independent of p_1^2 , and thereby the corresponding double discontinuity must vanish. As a result, the quark condensate contribution only comes from Fig. (4a).

E. Mixed quark-gluon condensate contribution

The quark-gluon condensate operator $\bar{q}g_s Gq$ has dimension 5 in OPE. There are three Feynman diagrams for mixed quark-gluon condensate contribution, as shown in Fig. 5. We are requested to consider the interaction of the propagating quark with the background gluons. The quark propagators with one gluon and two gluons attached (Fig. 6) respectively have the following forms:

$$S^{(1)ji}(x, y) = ig \int \frac{d^4 p_2}{(2\pi)^4} \int \frac{d^4 k}{(2\pi)^4} e^{-ip_2 \cdot y} e^{i(p_2 - k) \cdot x} \tilde{A}_{\mu}^{ji}(k) \frac{i}{\not{p}_2 - m} \gamma^{\mu} \frac{i}{\not{p}_2 - \not{k} - m},$$

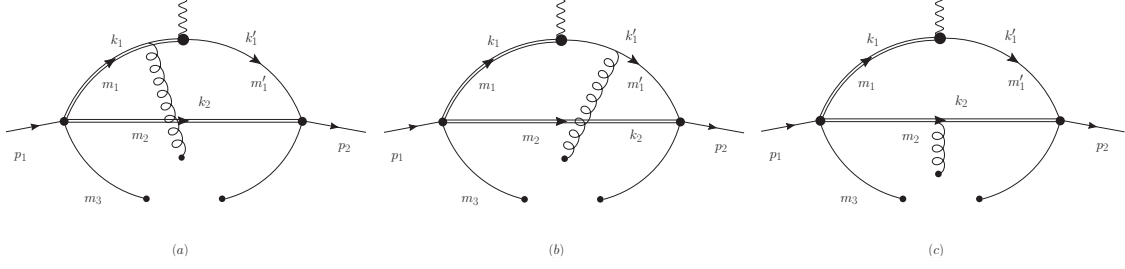
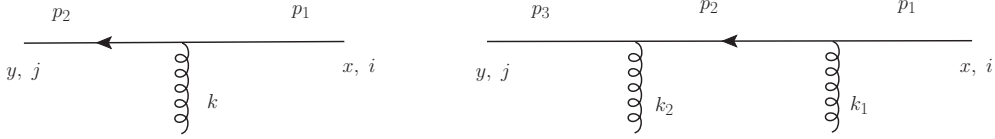


FIG. 5: Mixed quark-gluon condensate diagrams.

FIG. 6: Quark propagators in the QCD vacuum. x and y are spacetime coordinates, i and j are color indices, and p_i , k and k_i are momenta.

$$S^{(2)ji}(x, y) = (ig)^2 \int \frac{d^4 p_3}{(2\pi)^4} \int \frac{d^4 k_2}{(2\pi)^4} \int \frac{d^4 k_1}{(2\pi)^4} e^{-ip_3 \cdot y} e^{i(p_3 - k_2 - k_1) \cdot x} (\tilde{A}_\nu(k_2) \tilde{A}_\mu(k_1))^{ji} \\ \times \frac{i}{\not{p}_3 - m} \gamma^\nu \frac{i}{\not{p}_3 - \not{k}_2 - m} \gamma^\mu \frac{i}{\not{p}_3 - \not{k}_2 - \not{k}_1 - m}. \quad (29)$$

In the fixed-point gauge, the background gluon field expanded to the lowest order (in the momentum space) is:

$$\tilde{A}_\mu^a(k) = -\frac{i}{2} (2\pi)^4 G_{\alpha\mu}^a(0) \frac{\partial}{\partial k_\alpha} \delta^4(k). \quad (30)$$

Thus a propagating quark can exchange arbitrary numbers of zero momentum gluons with the QCD vacuum. It should be noted that the fixed-point gauge violates the spacetime translation invariance. As a result, $S(x, y)$ is not the same as $S(x - y, 0)$. In the cases of quark-gluon condensate contribution as well as gluon-gluon condensate contribution to be discussed in the following, the following formulas are useful:

$$\int d^4 u f(u) \frac{\partial}{\partial u_\alpha} \delta^4(u) = -\frac{\partial}{\partial u_\alpha} f(u) \Big|_{u=0}, \\ \frac{\partial}{\partial u_\alpha} \frac{1}{\not{p} + \not{u} - m} \Big|_{u=0} = -\frac{1}{\not{p} - m} \gamma^\alpha \frac{1}{\not{p} - m},$$

where u stands for the momentum of the soft gluon, and $f(u)$ is an arbitrary function of u .

In Fig (5a), the upper left heavy quark interacts with a background gluon field, which condensates with the two light quark fields. Its contribution is given as:

$$\Pi_\mu^{V, \langle \bar{q} G q \rangle, a}(p_1^2, p_2^2, q^2) = -\frac{\sqrt{2}}{192} \text{Tr}[T^a T^a] \langle \bar{q} g_s \sigma G q \rangle \int \frac{d^4 k_2}{(2\pi)^4} \frac{N_\mu^{V, \langle \bar{q} G q \rangle, a}}{(k_1^2 - m_1^2)^3 (k_1'^2 - m_1'^2) (k_2^2 - m_2^2)}. \quad (31)$$

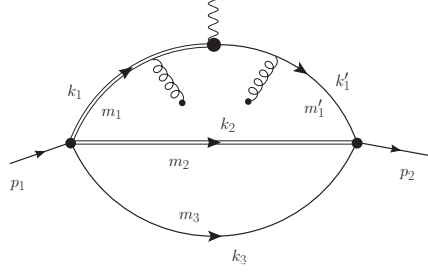


FIG. 7: One of the gluon-gluon condensate diagrams.

The condensate term is defined as $\langle q_a^i g_s G_{\mu\nu}^c \bar{q}_b^j \rangle = -(1/192) \langle \bar{q} g_s \sigma G q \rangle (\sigma_{\mu\nu})^{ij} T_{ab}^c$, and the numerator is:

$$N_{\mu}^{V, \langle \bar{q} G q \rangle, a} = \gamma_{\nu'} \gamma_5 (\not{k}_2 + m_2) \gamma^{\nu} (\not{k}_1 - m_1) \gamma^{\alpha} (\not{k}_1 - m_1) \gamma^{\rho} (\not{k}_1 - m_1) \gamma_{\mu} (\not{k}'_1 - m'_1) \gamma^{\nu'} \sigma_{\rho\alpha} \gamma_{\nu} \gamma_5, \\ k_1 = p_1 - k_2, \quad k'_1 = p_2 - k_2. \quad (32)$$

In Eq. (31), $1/(k_1^2 - m_1^2)^3$ can be handled in a derivative method:

$$\frac{1}{(k_1^2 - m_1^2)^n} = \frac{1}{(n-1)!} \frac{\partial^{n-1}}{(\partial m_{1s})^{n-1}} \left(\frac{1}{k_1^2 - m_{1s}} \right) \Big|_{m_{1s}=m_1^2}. \quad (33)$$

Then the spectral function can be derived by using Cutkosky rule before applying the mass derivative:

$$\rho_{\mu}^{V, \langle \bar{q} G q \rangle, a}(p_1^2, p_2^2, q^2) = \frac{(-2\pi i)^3}{(2\pi i)^2} \left(-\frac{\sqrt{2}}{192} \right) \text{Tr}[T^a T^a] \langle \bar{q} g_s \sigma G q \rangle \frac{1}{(2\pi)^4} \\ \times \left(\frac{1}{2} \frac{\partial^2}{(\partial m_{1s})^2} \int_{\Delta} N_{\mu}^{V, \langle \bar{q} G q \rangle, a} \Big|_{k_1^2 \rightarrow m_{1s}} \right) \Big|_{m_{1s} \rightarrow m_1^2}, \quad (34)$$

The the integral \int_{Δ} is slightly different from that in Eq. (27), with m_1^2 being replaced by m_{1s} . The other two diagrams in Fig. 5 can be calculated similarly.

F. Gluon-gluon condensate contribution

In the case of the dim-4 operator GG in the OPE, i.e. the gluon-gluon condensate, two background gluon fields interact with the four quark propagators, and one example is shown in Fig. 7.

The contribution from Fig. 7 is:

$$\Pi_{\mu}^{V, \langle GG \rangle}(p_1^2, p_2^2, q^2) = \frac{\langle g_s^2 GG \rangle}{48\sqrt{2}} \text{Tr}[T^a T^a] \int \frac{d^4 k_2}{(2\pi)^4} \frac{d^4 k_3}{(2\pi)^4} (-g_{\alpha\sigma} g_{\rho\beta} + g_{\alpha\beta} g_{\rho\sigma}) \\ \times \left(-\gamma_{\nu'} \gamma_5 \frac{1}{\not{k}_2 - m_2} \gamma^{\nu} \frac{1}{\not{k}_1 + m_1} \gamma^{\alpha} \frac{1}{\not{k}_1 + m_1} \gamma^{\rho} \frac{1}{\not{k}_1 + m_1} \right. \\ \left. \times \gamma_{\mu} \frac{1}{\not{k}'_1 + m'_1} \gamma^{\sigma} \frac{1}{\not{k}'_1 + m'_1} \gamma^{\beta} \frac{1}{\not{k}'_1 + m'_1} \gamma^{\nu'} \frac{1}{\not{k}_3 - m_3} \gamma_{\nu} \gamma_5 \right).$$

Note that $\Pi_\mu^{V,(GG)}(p_1^2, p_2^2, q^2)$ contains 19 Dirac matrices.

Similar procedure can be applied to extract the spectral function, and the corresponding numerical results will be shown in Sec. III.

III. NUMERICAL RESULTS

The input parameters used in our numerical calculation are taken as [50–53]: $\langle \bar{q}q \rangle = -(0.24 \pm 0.01 \text{ GeV})^3$, $\langle \bar{s}s \rangle = (0.8 \pm 0.2) \langle \bar{q}q \rangle$, $\langle \bar{q}g_s \sigma G q \rangle = m_0^2 \langle \bar{q}q \rangle$, $\langle \bar{s}g_s \sigma G s \rangle = m_0^2 \langle \bar{s}s \rangle$, $m_0^2 = (0.8 \pm 0.2) \text{ GeV}^2$, $\langle \frac{\alpha_s GG}{\pi} \rangle = (0.012 \pm 0.004) \text{ GeV}^4$ for the condensate parameters and $m_s = (0.14 \pm 0.01) \text{ GeV}$, $m_c = (1.35 \pm 0.10) \text{ GeV}$, $m_b = (4.7 \pm 0.1) \text{ GeV}$ for the quark masses. The pole residues of doubly-heavy and singly-heavy baryons as well as their masses are collected in Table II. The factor $\sqrt{2}$ in Table II arises from the convention difference in the definitions of the interpolating current for baryon [18, 54, 55]. For doubly-heavy baryons, we have updated the pole residues using the same inputs as those in this work. The mass of Ξ_{cc}^{++} comes from the experiment [1] and other masses of doubly heavy baryons are predictions of the Lattice QCD [56]. Masses for baryons with a single heavy quark are taken from Particle Data Group [52, 53]. Masses of the negative parity baryons presented in Eq. (17) are collected in Table III [49, 57].

When arriving at the predictions of the branching ratios, the lifetimes of the initial doubly-heavy baryons are also needed. They are collected in Table IV, in which the lifetime of Ξ_{cc}^{++} comes from the experiment [2], and other results are the theoretical predictions [45, 58, 59].

The threshold parameters $\sqrt{s_{1,2}^0}$ are taken from Table II, which are essentially about 0.5 GeV higher than the corresponding baryon mass [60]. We employ the following equation from Ref. [61] to simplify the selection of Borel mass parameters:

$$\frac{T_1^2}{T_2^2} \approx \frac{M_1^2 - m_1^2}{M_2^2 - m_1^2}, \quad (35)$$

where $M_{1(2)}$ is the mass of the initial (final) baryon and $m_1^{(\prime)}$ is the mass of the initial (final) quark. To determine the window of the Borel parameter T_1^2 , the criteria of pole dominance

$$r \equiv \frac{\int_0^{s_1^0} ds_1 \int_0^{s_2^0} ds_2 \rho^{\text{QCD}}(s_1, s_2, q^2) \exp(-s_1/T_1^2 - s_2/T_2^2)}{\int_0^\infty ds_1 \int_0^\infty ds_2 \rho^{\text{QCD}}(s_1, s_2, q^2) \exp(-s_1/T_1^2 - s_2/T_2^2)} \gtrsim 0.5 \quad (36)$$

and OPE convergence are invoked. For the latter, the reader can refer to Table VI. The obtained windows for T_1^2 can be seen in Table VII. In Table XIV, we have evaluated all the error sources for the form factors of $\Xi_{cc}^{++} \rightarrow \Sigma_c^+$. One can see that the Borel parameter dependence is weak.

More comments on the selection of the Borel parameters are in order. T_1^2 and T_2^2 are in fact free parameters in the dispersion integral. To investigate the dependence on the Borel parameters, we take the $\Xi_{cc}^{++} \rightarrow \Sigma_c^+$ process as an example. First, we calculate the form factors $F_{1,2,3}(0)$ as functions of T_1^2 and T_2^2 in the square region $[1, 10] \text{ GeV}^2 \times [1, 10] \text{ GeV}^2$. Then the obtained results are represented graphically in Fig. 8, where the positive and negative values are respectively

TABLE II: “Decay constants” (pole residues) for the doubly-heavy and singly-heavy hadrons as well as their masses. Results for charmed and bottom baryons are taken from Refs. [54, 55], while for doubly-heavy baryons, we have updated the pole residues in Ref. [18] using the same inputs as those in this work. The factor $\sqrt{2}$ arises from the convention differences in the definitions of the interpolating current for baryon. The mass of Ξ_{cc}^{++} comes from the experiment [1] and other masses of doubly heavy baryons are predictions of the Lattice QCD [56]. Masses for baryons with a single heavy quark are taken from Particle Data Group [52, 53].

	$T^2(\text{GeV}^2)$	$\sqrt{s_0}(\text{GeV})$	$M(\text{GeV})$	$\lambda(\text{GeV}^3)$
Λ_c	1.7 – 2.7	3.1 ± 0.1	2.286	$\sqrt{2}(0.022 \pm 0.003)$
Ξ_c	1.9 – 2.9	3.2 ± 0.1	2.468	$\sqrt{2}(0.027 \pm 0.004)$
Λ_b	4.3 – 5.3	6.5 ± 0.1	5.620	$\sqrt{2}(0.028 \pm 0.004)$
Ξ_b	4.4 – 5.4	6.5 ± 0.1	5.793	$\sqrt{2}(0.034 \pm 0.006)$
Σ_c	1.8 – 2.8	3.2 ± 0.1	2.454	$\sqrt{2}(0.046 \pm 0.006)$
Ξ'_c	2.0 – 3.0	3.3 ± 0.1	2.576	$\sqrt{2}(0.054 \pm 0.007)$
Ω_c	2.2 – 3.2	3.4 ± 0.1	2.695	0.089 ± 0.013
Σ_b	4.6 – 5.6	6.6 ± 0.1	5.814	$\sqrt{2}(0.062 \pm 0.010)$
Ξ'_b	4.9 – 5.9	6.7 ± 0.1	5.935	$\sqrt{2}(0.074 \pm 0.011)$
Ω_b	5.2 – 6.2	6.8 ± 0.1	6.046	0.123 ± 0.020
Ξ_{cc}	2.4 – 3.4	4.1 ± 0.1	3.621	0.109 ± 0.020
Ω_{cc}	2.6 – 3.6	4.3 ± 0.1	3.738 ± 0.028	0.129 ± 0.024
Ξ_{bb}	6.8 – 7.8	10.6 ± 0.1	10.143 ± 0.038	0.199 ± 0.052
Ω_{bb}	7.2 – 8.2	10.8 ± 0.1	10.273 ± 0.034	0.253 ± 0.062
Ξ_{bc}	4.2 – 5.2	7.4 ± 0.1	6.943 ± 0.043	0.150 ± 0.035
Ω_{bc}	4.5 – 5.5	7.6 ± 0.1	6.998 ± 0.034	0.168 ± 0.038

TABLE III: Masses (in units of GeV) of the negative parity baryons [49, 57].

Baryon	$\Xi_{cc}(\frac{1}{2}^-)$	$\Omega_{cc}(\frac{1}{2}^-)$	$\Xi_{bc}(\frac{1}{2}^-)$	$\Omega_{bc}(\frac{1}{2}^-)$	$\Xi_{bb}(\frac{1}{2}^-)$	$\Omega_{bb}(\frac{1}{2}^-)$
Mass	3.77 [49]	3.91 [49]	7.231 [57]	7.346 [57]	10.38 [49]	10.53 [49]
Baryon	$\Lambda_c(\frac{1}{2}^-)$	$\Xi_c(\frac{1}{2}^-)$	$\Sigma_c(\frac{1}{2}^-)$	$\Xi'_c(\frac{1}{2}^-)$	$\Omega_c(\frac{1}{2}^-)$	
Mass	2.592 [57]	2.789 [57]	2.74 [49]	2.87 [49]	2.98 [49]	
Baryon	$\Lambda_b(\frac{1}{2}^-)$	$\Xi_b(\frac{1}{2}^-)$	$\Sigma_b(\frac{1}{2}^-)$	$\Xi'_b(\frac{1}{2}^-)$	$\Omega_b(\frac{1}{2}^-)$	
Mass	5.912 [57]	6.108 [57]	6.00 [49]	6.14 [49]	6.27 [49]	

TABLE IV: Lifetimes (in units of fs) of doubly-heavy baryons. The lifetime of Ξ_{cc}^{++} comes from the experiment [2], and other results are theoretical predictions [45, 58, 59].

Baryon	Ξ_{cc}^{++}	Ξ_{cc}^+	Ω_{cc}^+	Ξ_{bc}^+	Ξ_{bc}^0	Ω_{bc}^0	Ξ_{bb}^0	Ξ_{bb}^-	Ω_{bb}^-
Lifetime	256 [2]	44 [59]	206 [59]	244 [58]	93 [58]	220 [45]	370 [58]	370 [58]	800 [45]

displayed as reddish and bluish, and the greater the absolute value for the form factors $F_{1,2,3}(0)$, the darker the color. In the end, the following three criteria are employed to determine the Borel region:

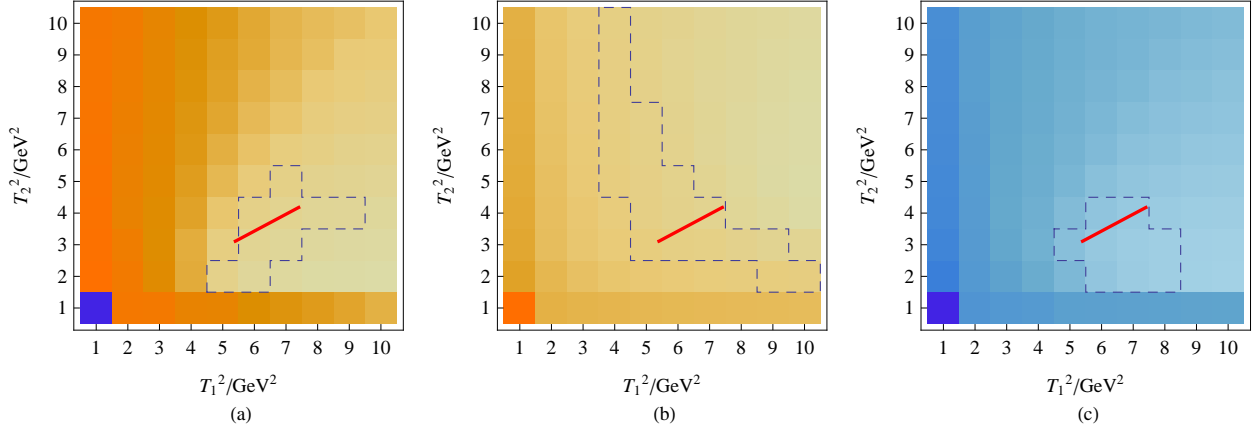


FIG. 8: $F_{1,2,3}$ at $q^2 = 0$ as functions of the Borel parameters T_1^2 and T_2^2 in the process of $\Xi_{cc}^{++} \rightarrow \Sigma_c^+$, where T_1^2 and T_2^2 are taken as free parameters. Positive and negative values are respectively displayed as reddish ($F_{1,2}$) and bluish (F_3), and the greater the absolute value for the form factors $F_i(0)$, the darker the color. The allowed Borel regions are enclosed by the dashed contours. To determine these regions, three criteria have been applied, as can be seen in the text. The red line segment determined by Eq. (35), which is adopted in this work, is also shown on each figure.

TABLE V: The quantitative criteria of the pole dominance and OPE convergence, and a comparison of the results of $F_i(0)$ obtained by these two different ways to determine Borel parameters. When the Borel parameters are taken as free, we average the values of $F_i(0)$ within the Borel region in Fig. 8, and when Eq. (35) is used, the value evaluated at the midpoint of the line segment in Fig. 8 is shown. The process of $\Xi_{cc}^{++} \rightarrow \Sigma_c^+$ is considered.

	$F_1(0)$	$F_2(0)$	$F_3(0)$
The pole dominance r	> 0.5	> 0.5	> 0.45
OPE convergence dim-5/total	$< 5\%$	$< 10\%$	$< 8\%$
Free Borel parameters	1.126	0.638	-2.008
Constrained Borel parameters	1.147	0.641	-2.059

- The pole dominance. See Eq. (36).
- OPE convergence. This can be achieved by demanding that the contribution from the quark-gluon condensate (dim-5) is less than, for example, 10%.
- Stability of the quantity within the Borel region. This can be read directly from Fig. 8.

More details can be found in Table V. In Fig. 8, we also show the line segment determined by Eq. (35). It can be seen that, the simplified Eq. (35) is still a good approximation, and a quantitative comparison between these two different ways to determine Borel parameters can be seen in Table V.

Numerical results for the form factors are given in Tables VIII, IX, X and XI for the doubly-charmed, doubly-bottom and bottom-charm baryons. In QCDSR, the OPE is applicable in the

TABLE VI: Contributions to form factors from dim-0, 3, 5 and the gluon-gluon condensate shown in Fig. 7 for the $\Xi_{cc}^{++} \rightarrow \Sigma_c^+$ transition with T_1^2 taking as the central value 5.9 GeV².

	$F_1(0)$	$F_2(0)$	$F_3(0)$	$G_1(0)$	$G_2(0)$	$G_3(0)$
dim-0	0.507	0.194	-0.824	-1.162	0.627	0.205
dim-3	0.606	0.391	-1.129	-1.605	1.099	0.211
dim-5	0.034	0.056	-0.106	-0.291	0.217	0.012
Fig. 7	-0.007	-0.008	0.012	--	--	--

TABLE VII: The windows of the Borel parameter T_1^2 and the range of r in Eq. (36) for the form factors in different transitions. T_2^2 is determined by Eq. (35). The momentum transfer squared q^2 is taken at -0.5 GeV² (-5 GeV²) for the case of c (b) quark decay. The central value of T_1^2 will be taken as the midpoint of the interval.

Transition	$T_1^2(\text{GeV}^2)$	F_1	F_2	F_3
$\Xi_{cc} \rightarrow \Sigma_c$	4.9 – 6.9	(61 – 82)%	(56 – 80)%	(51 – 76)%
$\Xi_{bc} \rightarrow \Sigma_b$	10.2 – 12.2	(70 – 93)%	(50 – 68)%	(54 – 75)%
$\Xi_{bc} \rightarrow \Sigma_c$	9.8 – 11.8	(53 – 70)%	(57 – 67)%	(50 – 61)%
$\Xi_{bb} \rightarrow \Sigma_b$	11.9 – 13.9	(51 – 58)%	(54 – 61)%	(50 – 57)%
$\Xi_{cc} \rightarrow \Lambda_c$	5.7 – 7.7	(86 – 90)%	(72 – 85)%	(51 – 73)%
$\Xi_{bc} \rightarrow \Lambda_b$	11.6 – 13.6	(72 – 89)%	(69 – 91)%	(51 – 68)%
$\Xi_{bc} \rightarrow \Lambda_c$	10.4 – 12.4	(65 – 70)%	(58 – 66)%	(50 – 60)%
$\Xi_{bb} \rightarrow \Lambda_b$	10.9 – 12.9	(51 – 59)%	(52 – 59)%	(50 – 57)%

deep Euclidean region, where $q^2 \ll 0$. In this work, we directly calculate the form factors in the region $-1 < q^2 < 0$ GeV² for the charm quark decay, and $0 < q^2 < 5$ GeV² for the bottom quark decay. In order to access the q^2 distribution in the full kinematic region, the form factors are extrapolated with a parametrization. We adopt the following double-pole parameterization:

$$F(q^2) = \frac{F(0)}{1 - \frac{q^2}{m_{\text{fit}}^2} + \delta \left(\frac{q^2}{m_{\text{fit}}^2} \right)^2}. \quad (37)$$

A few remarks are given in order.

- We have also calculated part of the gluon-gluon condensate, shown in Fig. 7, for $\Xi_{cc}^{++} \rightarrow \Sigma_c^+$, and make a comparison with other contributions in Table VI. From this table, it is plausible to conclude the following pattern:

$$\text{dim-0} \sim \text{dim-3} \gg \text{dim-5} \gg \text{dim-4}. \quad (38)$$

We intend to perform a more comprehensive analysis by including all the contributions from the gluon-gluon condensate in future.

TABLE VIII: The form factors for the cc sector. Eq. (37) is adopted as the fit formula. The results for $\Xi_{cc} \rightarrow \Sigma_c$ correspond to $\Xi_{cc}^{++} \rightarrow \Sigma_c^+$. A factor $\sqrt{2}$ should be multiplied to $F(0)$ for $\Xi_{cc}^+ \rightarrow \Sigma_c^0$. The form factor f_2 in the $\Xi_{cc} \rightarrow \Xi_c$ and $\Omega_{cc} \rightarrow \Xi_c$ transitions can not be fitted well, the corresponding (m_{fit}, δ) are taken from those in the $\Xi_{cc} \rightarrow \Lambda_c$ transition. For $F(0)$, we have only considered the uncertainty from the heavy quark masses.

F	$F(0)$	m_{fit}	δ	F	$F(0)$	m_{fit}	δ
$f_1^{\Xi_{cc} \rightarrow \Lambda_c}$	-0.63 ± 0.20	1.57	0.08	$g_1^{\Xi_{cc} \rightarrow \Lambda_c}$	0.24 ± 0.08	2.27	0.39
$f_2^{\Xi_{cc} \rightarrow \Lambda_c}$	0.05 ± 0.02	2.43	2.10	$g_2^{\Xi_{cc} \rightarrow \Lambda_c}$	-0.11 ± 0.03	1.54	0.12
$f_3^{\Xi_{cc} \rightarrow \Lambda_c}$	0.81 ± 0.26	1.34	0.20	$g_3^{\Xi_{cc} \rightarrow \Lambda_c}$	-0.84 ± 0.30	1.34	0.20
$f_1^{\Xi_{cc} \rightarrow \Xi_c}$	-0.69 ± 0.23	1.54	-0.01	$g_1^{\Xi_{cc} \rightarrow \Xi_c}$	0.25 ± 0.08	2.30	0.39
$f_2^{\Xi_{cc} \rightarrow \Xi_c}$	0.06 ± 0.02	2.43	2.10	$g_2^{\Xi_{cc} \rightarrow \Xi_c}$	-0.14 ± 0.04	1.54	0.21
$f_3^{\Xi_{cc} \rightarrow \Xi_c}$	0.91 ± 0.30	1.30	0.12	$g_3^{\Xi_{cc} \rightarrow \Xi_c}$	-0.92 ± 0.31	1.34	0.22
$f_1^{\Omega_{cc} \rightarrow \Xi_c}$	-0.67 ± 0.21	1.66	0.21	$g_1^{\Omega_{cc} \rightarrow \Xi_c}$	0.25 ± 0.08	2.34	0.38
$f_2^{\Omega_{cc} \rightarrow \Xi_c}$	0.06 ± 0.02	2.43	2.10	$g_2^{\Omega_{cc} \rightarrow \Xi_c}$	-0.12 ± 0.03	1.51	-0.05
$f_3^{\Omega_{cc} \rightarrow \Xi_c}$	0.84 ± 0.26	1.37	0.19	$g_3^{\Omega_{cc} \rightarrow \Xi_c}$	-0.89 ± 0.30	1.35	0.12
$f_1^{\Xi_{cc} \rightarrow \Sigma_c}$	-0.30 ± 0.07	1.76	-0.65	$g_1^{\Xi_{cc} \rightarrow \Sigma_c}$	0.46 ± 0.15	2.29	0.41
$f_2^{\Xi_{cc} \rightarrow \Sigma_c}$	1.05 ± 0.38	1.57	0.23	$g_2^{\Xi_{cc} \rightarrow \Sigma_c}$	-0.09 ± 0.01	1.20	1.59
$f_3^{\Xi_{cc} \rightarrow \Sigma_c}$	0.10 ± 0.00	1.00	0.78	$g_3^{\Xi_{cc} \rightarrow \Sigma_c}$	-2.96 ± 1.13	1.34	0.16
$f_1^{\Xi_{cc} \rightarrow \Xi'_c}$	-0.31 ± 0.06	2.25	1.08	$g_1^{\Xi_{cc} \rightarrow \Xi'_c}$	0.50 ± 0.17	2.28	0.42
$f_2^{\Xi_{cc} \rightarrow \Xi'_c}$	1.10 ± 0.40	1.54	0.12	$g_2^{\Xi_{cc} \rightarrow \Xi'_c}$	-0.17 ± 0.03	1.14	0.48
$f_3^{\Xi_{cc} \rightarrow \Xi'_c}$	0.15 ± 0.02	1.02	0.44	$g_3^{\Xi_{cc} \rightarrow \Xi'_c}$	-3.09 ± 1.18	1.34	0.15
$f_1^{\Omega_{cc} \rightarrow \Xi'_c}$	-0.28 ± 0.05	2.07	-0.60	$g_1^{\Omega_{cc} \rightarrow \Xi'_c}$	0.49 ± 0.16	2.20	-0.07
$f_2^{\Omega_{cc} \rightarrow \Xi'_c}$	1.13 ± 0.40	1.59	0.19	$g_2^{\Omega_{cc} \rightarrow \Xi'_c}$	-0.08 ± 0.01	1.22	2.60
$f_3^{\Omega_{cc} \rightarrow \Xi'_c}$	0.07 ± 0.00	1.15	4.13	$g_3^{\Omega_{cc} \rightarrow \Xi'_c}$	-3.20 ± 1.19	1.37	0.16
$f_1^{\Omega_{cc} \rightarrow \Omega_c}$	-0.42 ± 0.08	1.78	-0.96	$g_1^{\Omega_{cc} \rightarrow \Omega_c}$	0.74 ± 0.25	2.37	0.54
$f_2^{\Omega_{cc} \rightarrow \Omega_c}$	1.66 ± 0.58	1.65	0.36	$g_2^{\Omega_{cc} \rightarrow \Omega_c}$	-0.19 ± 0.03	1.59	3.77
$f_3^{\Omega_{cc} \rightarrow \Omega_c}$	0.16 ± 0.01	1.20	1.81	$g_3^{\Omega_{cc} \rightarrow \Omega_c}$	-4.72 ± 1.76	1.36	0.15

- The form factors g_i 's are determined in the following way. Rewrite Eq. (14) as

$$\Pi_{\mu}^{V,\text{pole}} = \sum_{i=1}^{12} A_i^V e_{i\mu}^V, \quad (39)$$

and similarly write the pole contribution for the axial-vector current correlation function as

$$\Pi_{\mu}^{A,\text{pole}} = \sum_{i=1}^{12} A_i^A e_{i\mu}^A, \quad (40)$$

where $e_{i\mu}^V \equiv e_{i\mu}$ in Eq. (15) and

$$\begin{aligned} (e_{1,2,3,4}^A)_{\mu} &\equiv \{\not{p}_2, 1\} \times \{p_{1\mu} \gamma_5\} \times \{\not{p}_1, 1\}, \\ (e_{5,6,7,8}^A)_{\mu} &\equiv \{\not{p}_2, 1\} \times \{p_{2\mu} \gamma_5\} \times \{\not{p}_1, 1\}, \\ (e_{9,10,11,12}^A)_{\mu} &\equiv \{\not{p}_2, 1\} \times \{\gamma_{\mu} \gamma_5\} \times \{\not{p}_1, 1\}. \end{aligned} \quad (41)$$

TABLE IX: The form factors for the bb sector. Eq. (37) is adopted as the fit formula. The results for $\Xi_{bb}^- \rightarrow \Sigma_b^-$ correspond to $\Xi_{bb}^- \rightarrow \Sigma_b^0$. A factor $\sqrt{2}$ should be multiplied to $F(0)$ for $\Xi_{bb}^0 \rightarrow \Sigma_b^+$. For $F(0)$, we have only considered the uncertainty from the heavy quark masses.

F	$F(0)$	m_{fit}	δ	F	$F(0)$	m_{fit}	δ
$f_1^{\Xi_{bb}^- \rightarrow \Lambda_b}$	-0.072 ± 0.041	2.52	0.39	$g_1^{\Xi_{bb}^- \rightarrow \Lambda_b}$	0.027 ± 0.015	2.65	0.41
$f_2^{\Xi_{bb}^- \rightarrow \Lambda_b}$	0.004 ± 0.003	2.62	0.40	$g_2^{\Xi_{bb}^- \rightarrow \Lambda_b}$	-0.013 ± 0.007	2.47	0.39
$f_3^{\Xi_{bb}^- \rightarrow \Lambda_b}$	0.085 ± 0.048	2.41	0.37	$g_3^{\Xi_{bb}^- \rightarrow \Lambda_b}$	-0.069 ± 0.040	2.42	0.37
$f_1^{\Omega_{bb}^- \rightarrow \Xi_b^-}$	-0.095 ± 0.053	2.66	0.35	$g_1^{\Omega_{bb}^- \rightarrow \Xi_b^-}$	0.036 ± 0.021	2.81	0.36
$f_2^{\Omega_{bb}^- \rightarrow \Xi_b^-}$	0.006 ± 0.004	2.72	0.37	$g_2^{\Omega_{bb}^- \rightarrow \Xi_b^-}$	-0.017 ± 0.009	2.60	0.35
$f_3^{\Omega_{bb}^- \rightarrow \Xi_b^-}$	0.112 ± 0.063	2.52	0.35	$g_3^{\Omega_{bb}^- \rightarrow \Xi_b^-}$	-0.093 ± 0.053	2.53	0.35
$f_1^{\Xi_{bb}^- \rightarrow \Sigma_b^-}$	-0.050 ± 0.026	2.89	0.38	$g_1^{\Xi_{bb}^- \rightarrow \Sigma_b^-}$	0.060 ± 0.032	2.96	0.39
$f_2^{\Xi_{bb}^- \rightarrow \Sigma_b^-}$	0.149 ± 0.082	2.65	0.37	$g_2^{\Xi_{bb}^- \rightarrow \Sigma_b^-}$	0.016 ± 0.008	3.24	0.75
$f_3^{\Xi_{bb}^- \rightarrow \Sigma_b^-}$	0.012 ± 0.005	2.35	0.34	$g_3^{\Xi_{bb}^- \rightarrow \Sigma_b^-}$	-0.377 ± 0.205	2.60	0.36
$f_1^{\Omega_{bb}^- \rightarrow \Xi_b^{\prime -}}$	-0.057 ± 0.028	2.97	0.39	$g_1^{\Omega_{bb}^- \rightarrow \Xi_b^{\prime -}}$	0.072 ± 0.037	2.99	0.41
$f_2^{\Omega_{bb}^- \rightarrow \Xi_b^{\prime -}}$	0.180 ± 0.095	2.70	0.37	$g_2^{\Omega_{bb}^- \rightarrow \Xi_b^{\prime -}}$	0.019 ± 0.010	3.69	0.89
$f_3^{\Omega_{bb}^- \rightarrow \Xi_b^{\prime -}}$	0.012 ± 0.005	2.27	0.36	$g_3^{\Omega_{bb}^- \rightarrow \Xi_b^{\prime -}}$	-0.453 ± 0.234	2.65	0.37

In the massless limit $m'_1 \rightarrow 0$ and $m_3 \rightarrow 0$, one can prove for the process of the final baryon belonging to the sextet:

$$\begin{aligned}
A_i^{A,\text{dim-0}} &= -A_i^{V,\text{dim-0}}, & A_i^{A,\text{dim-3}} &= A_i^{V,\text{dim-3}}, & A_i^{A,\text{dim-5}} &= A_i^{V,\text{dim-5}}, & \text{for } i \text{ odd,} \\
A_i^{A,\text{dim-0}} &= A_i^{V,\text{dim-0}}, & A_i^{A,\text{dim-3}} &= -A_i^{V,\text{dim-3}}, & A_i^{A,\text{dim-5}} &= -A_i^{V,\text{dim-5}}, & \text{for } i \text{ even,}
\end{aligned} \quad (42)$$

and for the process of the final baryon belonging to the anti-triplet:

$$\begin{aligned}
A_i^{A,\text{dim-0}} &= A_i^{V,\text{dim-0}}, & A_i^{A,\text{dim-3}} &= -A_i^{V,\text{dim-3}}, & A_i^{A,\text{dim-5}} &= -A_i^{V,\text{dim-5}}, & \text{for } i \text{ odd,} \\
A_i^{A,\text{dim-0}} &= -A_i^{V,\text{dim-0}}, & A_i^{A,\text{dim-3}} &= A_i^{V,\text{dim-3}}, & A_i^{A,\text{dim-5}} &= A_i^{V,\text{dim-5}}, & \text{for } i \text{ even.}
\end{aligned} \quad (43)$$

Here $A_i^{A,\text{dim-0}}$ stands for the coefficient A_i^A in Eq. (40) with the dim-0 correlation function being considered only, and so forth.

- The uncertainties of form factors arise from those from the heavy quark masses, Borel parameter T_1^2 , thresholds s_1^0 and s_2^0 , condensate parameters, pole residues and masses of initial and final baryons. A detail analysis can be found in Subsection III A and Table XIV. It can be seen from XIV that, the uncertainty mainly comes from that of the heavy quark mass. Thus, in Tables VIII, IX, X and XI, we only list the uncertainties from the heavy quark masses.
- In Table VIII, the $\Xi_{cc} \rightarrow \Sigma_c$ stands for the $\Xi_{cc}^{++} \rightarrow \Sigma_c^+$ transition. A factor $\sqrt{2}$ should be added for the $\Xi_{cc}^+ \rightarrow \Sigma_c^0$ transition. This is consistent with the analysis based on the flavor SU(3) symmetry [8]. Similar arguments can also be found in Tables IX, X, and XI.

TABLE X: The form factors for the bc sector with c quark decay. Eq. (37) is adopted as the fit formula. The results for $\Xi_{bc} \rightarrow \Sigma_b$ correspond to $\Xi_{bc}^+ \rightarrow \Sigma_b^0$. A factor $\sqrt{2}$ should be multiplied to $F(0)$ for $\Xi_{bc}^0 \rightarrow \Sigma_b^-$. The form factors f_1, g_1 and g_2 in the $\Xi_{bc} \rightarrow \Xi'_b$ transition can not be fitted well, the corresponding (m_{fit}, δ) are taken from those in the $\Xi_{bc} \rightarrow \Sigma_b$ transition. Also, the form factor f_1 in the $\Omega_{bc} \rightarrow \Omega_b$ transition can not be fitted well, the corresponding (m_{fit}, δ) are taken from those in the $\Omega_{bc} \rightarrow \Xi'_b$ transition. For $F(0)$, we have only considered the uncertainty from the heavy quark masses.

F	$F(0)$	m_{fit}	δ	F	$F(0)$	m_{fit}	δ
$f_1^{\Xi_{bc} \rightarrow \Lambda_b}$	-0.45 ± 0.15	1.33	0.06	$g_1^{\Xi_{bc} \rightarrow \Lambda_b}$	0.16 ± 0.05	1.88	0.49
$f_2^{\Xi_{bc} \rightarrow \Lambda_b}$	0.31 ± 0.09	1.58	0.47	$g_2^{\Xi_{bc} \rightarrow \Lambda_b}$	-0.14 ± 0.04	1.28	0.61
$f_3^{\Xi_{bc} \rightarrow \Lambda_b}$	1.21 ± 0.37	1.23	0.27	$g_3^{\Xi_{bc} \rightarrow \Lambda_b}$	-2.74 ± 0.83	1.32	0.23
$f_1^{\Xi_{bc} \rightarrow \Xi_b}$	-0.45 ± 0.14	1.42	0.26	$g_1^{\Xi_{bc} \rightarrow \Xi_b}$	0.16 ± 0.05	1.90	0.45
$f_2^{\Xi_{bc} \rightarrow \Xi_b}$	0.32 ± 0.10	1.46	0.11	$g_2^{\Xi_{bc} \rightarrow \Xi_b}$	-0.15 ± 0.05	1.18	0.28
$f_3^{\Xi_{bc} \rightarrow \Xi_b}$	1.23 ± 0.38	1.24	0.28	$g_3^{\Xi_{bc} \rightarrow \Xi_b}$	-2.79 ± 0.83	1.31	0.21
$f_1^{\Omega_{bc} \rightarrow \Xi_b}$	-0.44 ± 0.13	1.44	0.21	$g_1^{\Omega_{bc} \rightarrow \Xi_b}$	0.16 ± 0.05	1.95	0.48
$f_2^{\Omega_{bc} \rightarrow \Xi_b}$	0.31 ± 0.09	1.54	0.20	$g_2^{\Omega_{bc} \rightarrow \Xi_b}$	-0.12 ± 0.04	1.18	0.32
$f_3^{\Omega_{bc} \rightarrow \Xi_b}$	1.12 ± 0.33	1.28	0.29	$g_3^{\Omega_{bc} \rightarrow \Xi_b}$	-2.62 ± 0.76	1.38	0.25
$f_1^{\Xi_{bc} \rightarrow \Sigma_b}$	-0.23 ± 0.06	1.70	0.67	$g_1^{\Xi_{bc} \rightarrow \Sigma_b}$	0.33 ± 0.11	1.73	0.13
$f_2^{\Xi_{bc} \rightarrow \Sigma_b}$	1.51 ± 0.50	1.39	0.24	$g_2^{\Xi_{bc} \rightarrow \Sigma_b}$	-0.39 ± 0.12	1.09	0.13
$f_3^{\Xi_{bc} \rightarrow \Sigma_b}$	0.38 ± 0.11	1.04	0.25	$g_3^{\Xi_{bc} \rightarrow \Sigma_b}$	-8.24 ± 2.97	1.24	0.31
$f_1^{\Xi_{bc} \rightarrow \Xi'_b}$	-0.24 ± 0.06	1.70	0.67	$g_1^{\Xi_{bc} \rightarrow \Xi'_b}$	0.35 ± 0.11	1.73	0.13
$f_2^{\Xi_{bc} \rightarrow \Xi'_b}$	1.56 ± 0.51	1.48	0.51	$g_2^{\Xi_{bc} \rightarrow \Xi'_b}$	-0.46 ± 0.12	1.09	0.13
$f_3^{\Xi_{bc} \rightarrow \Xi'_b}$	0.43 ± 0.12	1.09	0.30	$g_3^{\Xi_{bc} \rightarrow \Xi'_b}$	-8.44 ± 3.09	1.23	0.23
$f_1^{\Omega_{bc} \rightarrow \Xi'_b}$	-0.23 ± 0.07	1.66	0.31	$g_1^{\Omega_{bc} \rightarrow \Xi'_b}$	0.34 ± 0.11	1.89	0.43
$f_2^{\Omega_{bc} \rightarrow \Xi'_b}$	1.56 ± 0.50	1.45	0.30	$g_2^{\Omega_{bc} \rightarrow \Xi'_b}$	-0.34 ± 0.09	1.23	0.34
$f_3^{\Omega_{bc} \rightarrow \Xi'_b}$	0.35 ± 0.09	1.10	0.31	$g_3^{\Omega_{bc} \rightarrow \Xi'_b}$	-8.55 ± 2.93	1.28	0.34
$f_1^{\Omega_{bc} \rightarrow \Omega_b}$	-0.32 ± 0.07	1.66	0.31	$g_1^{\Omega_{bc} \rightarrow \Omega_b}$	0.51 ± 0.17	1.95	0.59
$f_2^{\Omega_{bc} \rightarrow \Omega_b}$	2.29 ± 0.74	1.46	0.28	$g_2^{\Omega_{bc} \rightarrow \Omega_b}$	-0.60 ± 0.18	1.21	0.28
$f_3^{\Omega_{bc} \rightarrow \Omega_b}$	0.58 ± 0.17	1.08	0.24	$g_3^{\Omega_{bc} \rightarrow \Omega_b}$	-12.50 ± 4.38	1.24	0.21

A comparison between this work and other works in the literature can be found in Tables XII and XIII for the cc sector, the bb sector and the bc sector with c or b quark decay.

Some comments:

- The signs of the form factors of $c \rightarrow d$ processes ($\Xi_{cc}^{++}(ccu) \rightarrow \Lambda_c^+(dcu)$ and $\Xi_{bc}^+(cbu) \rightarrow \Lambda_b^0(dbu)$) in the LFQM have been flipped so that those of vector-current form factors are the same as ours. This stems from the asymmetry of u and d in the wave-function of $\Lambda_Q = (1/\sqrt{2})(ud - du)Q$ with $Q = c/b$ in the final state.
- It can be seen from Tables XII and XIII that, most of our results are comparable with others in other literature up to a sign difference for the axial-vector current form factors. However, this will not affect our predictions on physical observables, see Sec. IV.

TABLE XI: The form factors for the bc sector with b quark decay. Eq. (37) is adopted as the fit formula. The results for $\Xi_{bc} \rightarrow \Sigma_c$ correspond to $\Xi_{bc}^0 \rightarrow \Sigma_c^+$. A factor $\sqrt{2}$ should be multiplied to $F(0)$ for $\Xi_{bc}^+ \rightarrow \Sigma_c^{++}$. The form factor g_1 in the $\Xi_{bc} \rightarrow \Lambda_c$ transition can not be fitted well, the corresponding (m_{fit}, δ) are taken from those in the $\Omega_{bc} \rightarrow \Xi_c$ transition. For $F(0)$, we have only considered the uncertainty from the heavy quark masses.

F	$F(0)$	m_{fit}	δ	F	$F(0)$	m_{fit}	δ
$f_1^{\Xi_{bc} \rightarrow \Lambda_c}$	-0.141 ± 0.052	3.56	0.28	$g_1^{\Xi_{bc} \rightarrow \Lambda_c}$	0.067 ± 0.024	4.06	0.37
$f_2^{\Xi_{bc} \rightarrow \Lambda_c}$	-0.040 ± 0.015	3.42	0.34	$g_2^{\Xi_{bc} \rightarrow \Lambda_c}$	-0.037 ± 0.013	3.62	0.37
$f_3^{\Xi_{bc} \rightarrow \Lambda_c}$	0.108 ± 0.039	3.29	0.34	$g_3^{\Xi_{bc} \rightarrow \Lambda_c}$	-0.006 ± 0.003	2.25	0.36
$f_1^{\Omega_{bc} \rightarrow \Xi_c}$	-0.172 ± 0.059	3.64	0.33	$g_1^{\Omega_{bc} \rightarrow \Xi_c}$	0.079 ± 0.027	4.06	0.37
$f_2^{\Omega_{bc} \rightarrow \Xi_c}$	-0.047 ± 0.017	3.53	0.34	$g_2^{\Omega_{bc} \rightarrow \Xi_c}$	-0.043 ± 0.014	3.80	0.36
$f_3^{\Omega_{bc} \rightarrow \Xi_c}$	0.130 ± 0.044	3.38	0.34	$g_3^{\Omega_{bc} \rightarrow \Xi_c}$	-0.011 ± 0.004	2.42	0.37
$f_1^{\Xi_{bc} \rightarrow \Sigma_c}$	-0.069 ± 0.022	4.84	0.40	$g_1^{\Xi_{bc} \rightarrow \Sigma_c}$	0.088 ± 0.032	4.71	0.38
$f_2^{\Xi_{bc} \rightarrow \Sigma_c}$	0.159 ± 0.058	3.52	0.33	$g_2^{\Xi_{bc} \rightarrow \Sigma_c}$	0.059 ± 0.021	3.79	0.41
$f_3^{\Xi_{bc} \rightarrow \Sigma_c}$	-0.036 ± 0.015	3.88	0.44	$g_3^{\Xi_{bc} \rightarrow \Sigma_c}$	-0.257 ± 0.089	3.42	0.34
$f_1^{\Omega_{bc} \rightarrow \Xi'_c}$	-0.076 ± 0.022	5.08	0.33	$g_1^{\Omega_{bc} \rightarrow \Xi'_c}$	0.101 ± 0.035	4.77	0.31
$f_2^{\Omega_{bc} \rightarrow \Xi'_c}$	0.179 ± 0.062	3.60	0.34	$g_2^{\Omega_{bc} \rightarrow \Xi'_c}$	0.063 ± 0.021	3.99	0.43
$f_3^{\Omega_{bc} \rightarrow \Xi'_c}$	-0.040 ± 0.016	4.02	0.46	$g_3^{\Omega_{bc} \rightarrow \Xi'_c}$	-0.286 ± 0.093	3.51	0.34

- The sign conventions for f_2 and g_2 in Refs. [62, 63] are different from ours in Eq. (2).

A. Uncertainties

In this subsection, we will investigate the dependence of the form factors on the inputs. $\Xi_{cc}^{++} \rightarrow \Sigma_c^+$ is taken as an example. In Table XIV, we have considered all the error sources including those from the heavy quark masses, Borel parameter T_1^2 , thresholds s_1^0 and s_2^0 , condensate parameters, pole residues and masses of initial and final baryons. One can see that the uncertainty mainly comes from that of the heavy quark mass m_c . That is, the results of the QCD sum rules are sensitive to the choice of the heavy quark mass. Similar situations are also encountered in studying other properties of heavy hadrons using QCD sum rules. In principle, this can be cured by calculating the contributions from the radiation corrections, which is undoubtedly a great challenge in the application of QCD sum rules. In this work, we will have to be content with the leading order results. Also note that the dependence of the form factors on Borel parameter T_1^2 is weak.

When all uncertainties are considered, from Table XIV, the error estimates of the form factors at $q^2 = 0$ for $\Xi_{cc}^{++} \rightarrow \Sigma_c^+$ transition turn out to be

$$\begin{aligned}
 f_1(0) &= -0.30 \pm 0.10, & f_2(0) &= 1.05 \pm 0.44, & f_3(0) &= 0.10 \pm 0.06, \\
 g_1(0) &= 0.46 \pm 0.18, & g_2(0) &= -0.09 \pm 0.06, & g_3(0) &= -2.96 \pm 1.30.
 \end{aligned}
 \tag{44}$$

TABLE XII: Comparison with the results of the light-front quark model (LFQM) [6], the nonrelativistic quark model (NRQM) and the MIT bag model (MBM) [62] for the form factors of $\Xi_{cc}^{++} \rightarrow \Lambda_c^+$ and $\Xi_{cc}^{++} \rightarrow \Sigma_c^+$. The signs of the form factors of $\Xi_{cc}^{++} \rightarrow \Lambda_c^+$ in the LFQM have been flipped so that those of vector-current form factors are the same as ours. For the same reason, all the results from NRQM and MBM are multiplied by -1 except for f_2 and g_2 , whose sign conventions in Ref. [62] are different from ours.

Transition	$F(0)$	This work	LFQM [6]	NRQM [62]	MBM [62]
$\Xi_{cc}^{++} \rightarrow \Lambda_c^+$	$f_1(0)$	-0.63	-0.79	-0.36	-0.45
	$f_2(0)$	0.05	0.01	-0.14	-0.01
	$f_3(0)$	0.81	--	-0.08	0.28
	$g_1(0)$	0.24	-0.22	-0.20	-0.15
	$g_2(0)$	-0.11	0.05	-0.01	-0.01
	$g_3(0)$	-0.84	--	0.03	0.70
$\Xi_{cc}^{++} \rightarrow \Sigma_c^+$	$f_1(0)$	-0.30	-0.47	-0.28	-0.30
	$f_2(0)$	1.05	1.04	0.14	0.91
	$f_3(0)$	0.10	--	-0.10	0.07
	$g_1(0)$	0.46	-0.62	-0.70	-0.56
	$g_2(0)$	-0.09	0.05	-0.02	0.05
	$g_3(0)$	-2.96	--	0.10	2.59

TABLE XIII: Comparison with the results of the light-front quark model (LFQM) [6] for the form factors of $\Xi_{bb}^- \rightarrow \Lambda_b^0, \Sigma_b^0$, $\Xi_{bc}^+ \rightarrow \Lambda_b^0, \Sigma_b^0$, and $\Xi_{bc}^0 \rightarrow \Lambda_c^+, \Sigma_c^+$. The signs of the form factors of $\Xi_{bc}^+ \rightarrow \Lambda_b^0$ in the LFQM have been flipped so that those of vector-current form factors are the same as ours.

Transition	$F(0)$	This work	LFQM [6]	Transition	$F(0)$	This work	LFQM [6]
$\Xi_{bb}^- \rightarrow \Lambda_b^0$	$f_1(0)$	-0.072	-0.102	$\Xi_{bb}^- \rightarrow \Sigma_b^0$	$f_1(0)$	-0.050	-0.060
	$f_2(0)$	0.004	0.001		$f_2(0)$	0.149	0.150
	$f_3(0)$	0.085	--		$f_3(0)$	0.012	--
	$g_1(0)$	0.027	-0.036		$g_1(0)$	0.060	-0.089
	$g_2(0)$	-0.013	0.012		$g_2(0)$	0.016	-0.017
	$g_3(0)$	-0.069	--		$g_3(0)$	-0.377	--
$\Xi_{bc}^+ \rightarrow \Lambda_b^0$	$f_1(0)$	-0.45	-0.55	$\Xi_{bc}^+ \rightarrow \Sigma_b^0$	$f_1(0)$	-0.23	-0.32
	$f_2(0)$	0.31	0.30		$f_2(0)$	1.51	1.54
	$f_3(0)$	1.21	--		$f_3(0)$	0.38	--
	$g_1(0)$	0.16	-0.15		$g_1(0)$	0.33	-0.41
	$g_2(0)$	-0.14	0.10		$g_2(0)$	-0.39	0.18
	$g_3(0)$	-2.74	--		$g_3(0)$	-8.24	--
$\Xi_{bc}^0 \rightarrow \Lambda_c^+$	$f_1(0)$	-0.141	-0.113	$\Xi_{bc}^0 \rightarrow \Sigma_c^+$	$f_1(0)$	-0.069	-0.071
	$f_2(0)$	-0.040	-0.030		$f_2(0)$	0.159	0.098
	$f_3(0)$	0.108	--		$f_3(0)$	-0.036	--
	$g_1(0)$	0.067	-0.047		$g_1(0)$	0.088	-0.103
	$g_2(0)$	-0.037	0.021		$g_2(0)$	0.059	-0.003
	$g_3(0)$	-0.006	--		$g_3(0)$	-0.257	--

TABLE XIV: The error estimates of the form factors for $\Xi_{cc}^{++} \rightarrow \Sigma_c^+$.

		Central value	m_c	s_1^0	s_2^0	T_1^2	λ_i	λ_f	M_1^-	M_2^-	$\langle \bar{q}q \rangle$	$\langle \bar{q}g_s\sigma Gq \rangle$
f_1	$f_1(0)$	-0.30	0.07	0.01	0.02	0.02	0.05	0.03	0.01	0.00	0.02	0.00
	m_{pole}	1.76	0.18	0.27	0.36	0.03	0.00	0.00	0.01	0.01	0.04	0.02
	δ	-0.65	0.67	0.43	1.03	0.21	0.00	0.00	0.00	0.01	0.04	0.04
f_2	$f_2(0)$	1.05	0.38	0.02	0.05	0.04	0.16	0.12	0.00	0.00	0.08	0.02
	m_{pole}	1.57	0.01	0.02	0.03	0.02	0.00	0.00	0.00	0.00	0.01	0.01
	δ	0.23	0.01	0.00	0.10	0.04	0.00	0.00	0.00	0.00	0.00	0.01
f_3	$f_3(0)$	0.10	0.00	0.02	0.04	0.02	0.02	0.01	0.02	0.02	0.00	0.01
	m_{pole}	1.00	0.08	0.04	0.01	0.02	0.00	0.00	0.05	0.00	0.00	0.01
	δ	0.78	0.43	0.58	0.34	0.10	0.00	0.00	0.39	0.07	0.05	0.15
g_1	$g_1(0)$	0.46	0.15	0.01	0.03	0.00	0.07	0.05	0.01	0.01	0.03	0.00
	m_{pole}	2.29	0.00	0.18	0.04	0.06	0.00	0.00	0.08	0.04	0.07	0.05
	δ	0.41	0.09	0.59	0.19	0.02	0.00	0.00	0.10	0.05	0.03	0.02
g_2	$g_2(0)$	-0.09	0.01	0.03	0.05	0.01	0.01	0.01	0.01	0.00	0.00	0.01
	m_{pole}	1.20	0.06	0.13	0.10	0.00	0.00	0.00	0.01	0.00	0.00	0.02
	δ	1.59	0.92	2.98	1.00	0.32	0.00	0.00	0.39	0.14	0.19	0.35
g_3	$g_3(0)$	-2.96	1.13	0.04	0.13	0.07	0.46	0.34	0.00	0.01	0.21	0.13
	m_{pole}	1.34	0.05	0.03	0.00	0.02	0.00	0.00	0.00	0.00	0.01	0.00
	δ	0.16	0.04	0.03	0.02	0.02	0.00	0.00	0.00	0.00	0.00	0.00

IV. PHENOMENOLOGICAL APPLICATIONS

In this section, results for form factors will be applied to calculate the partial widths of semileptonic decays.

A. Semi-leptonic decays

The effective Hamiltonian for the semi-leptonic process reads

$$\begin{aligned} \mathcal{H}_{\text{eff}} = & \frac{G_F}{\sqrt{2}} \left(V_{cs}^* [\bar{s}\gamma_\mu(1-\gamma_5)c][\bar{\nu}\gamma^\mu(1-\gamma_5)l] + V_{cd}^* [\bar{d}\gamma_\mu(1-\gamma_5)c][\bar{\nu}\gamma^\mu(1-\gamma_5)l] \right) \\ & + \frac{G_F}{\sqrt{2}} V_{ub} [\bar{u}\gamma_\mu(1-\gamma_5)b][\bar{l}\gamma^\mu(1-\gamma_5)\nu], \end{aligned} \quad (45)$$

where G_F is Fermi constant and $V_{cs,cd,ub}$ are Cabibbo-Kobayashi-Maskawa (CKM) matrix elements.

The helicity amplitudes will be used in the calculation and for the vector current and the axial-vector current, they are given as follows:

$$\begin{aligned} H_{\frac{1}{2},0}^V &= -i\frac{\sqrt{Q_-}}{\sqrt{q^2}} \left((M_1 + M_2)f_1 - \frac{q^2}{M_1}f_2 \right), & H_{\frac{1}{2},0}^A &= -i\frac{\sqrt{Q_+}}{\sqrt{q^2}} \left((M_1 - M_2)g_1 + \frac{q^2}{M}g_2 \right), \\ H_{\frac{1}{2},1}^V &= i\sqrt{2Q_-} \left(-f_1 + \frac{M_1 + M_2}{M}f_2 \right), & H_{\frac{1}{2},1}^A &= i\sqrt{2Q_+} \left(-g_1 - \frac{M_1 - M_2}{M_1}g_2 \right), \end{aligned}$$

$$H_{\frac{1}{2},t}^V = -i\frac{\sqrt{Q_+}}{\sqrt{q^2}} \left((M_1 - M_2)f_1 + \frac{q^2}{M_1}f_3 \right), \quad H_{\frac{1}{2},t}^A = -i\frac{\sqrt{Q_-}}{\sqrt{q^2}} \left((M_1 + M_2)g_1 - \frac{q^2}{M_1}g_3 \right), \quad (46)$$

where $Q_{\pm} = (M_1 \pm M_2)^2 - q^2$ and $M_{1(2)}$ is the mass of the initial (final) baryon. The amplitudes for negative helicity are given by

$$H_{-\lambda_2,-\lambda_W}^V = H_{\lambda_2,\lambda_W}^V \quad \text{and} \quad H_{-\lambda_2,-\lambda_W}^A = -H_{\lambda_2,\lambda_W}^A, \quad (47)$$

where λ_2 and λ_W denote the polarizations of the final baryon and the intermediate W boson, respectively. Then the helicity amplitudes for the $V - A$ current are obtained as

$$H_{\lambda_2,\lambda_W} = H_{\lambda_2,\lambda_W}^V - H_{\lambda_2,\lambda_W}^A. \quad (48)$$

Decay widths for $\mathcal{B}_1 \rightarrow \mathcal{B}_2 l \nu$ with the longitudinally and transversely polarized $l\nu$ pair are evaluated as

$$\frac{d\Gamma_L}{dq^2} = \frac{G_F^2 |V_{CKM}|^2 q^2 p (1 - \hat{m}_l^2)^2}{384\pi^3 M_1^2} \left((2 + \hat{m}_l^2)(|H_{-\frac{1}{2},0}|^2 + |H_{\frac{1}{2},0}|^2) + 3\hat{m}_l^2(|H_{-\frac{1}{2},t}|^2 + |H_{\frac{1}{2},t}|^2) \right), \quad (49)$$

$$\frac{d\Gamma_T}{dq^2} = \frac{G_F^2 |V_{CKM}|^2 q^2 p (1 - \hat{m}_l^2)^2 (2 + \hat{m}_l^2)}{384\pi^3 M_1^2} (|H_{\frac{1}{2},1}|^2 + |H_{-\frac{1}{2},-1}|^2), \quad (50)$$

where $\hat{m}_l \equiv m_l/\sqrt{q^2}$, $p = \sqrt{Q_+Q_-}/(2M_1)$ is the magnitude of three-momentum of \mathcal{B}_2 in the rest frame of \mathcal{B}_1 . Integrating out the squared momentum transfer q^2 , we obtain the total decay width:

$$\Gamma = \int_{m_l^2}^{(M_1-M_2)^2} dq^2 \frac{d\Gamma}{dq^2}, \quad (51)$$

where

$$\frac{d\Gamma}{dq^2} = \frac{d\Gamma_L}{dq^2} + \frac{d\Gamma_T}{dq^2}. \quad (52)$$

The Fermi constant and CKM matrix elements are taken from Particle Data Group [52, 53]:

$$G_F = 1.166 \times 10^{-5} \text{GeV}^{-2},$$

$$|V_{cd}| = 0.225, \quad |V_{cs}| = 0.974, \quad |V_{ub}| = 0.00357. \quad (53)$$

The lifetimes of the doubly heavy baryons are given in Table IV. The integrated partial decay widths, ratios of Γ_L/Γ_T and the corresponding branching fractions are calculated and results are given in Tables XV, XVI, XVII and XVIII respectively. A comparison of our results with those in the literature is presented in Table XIX.

A few remarks are given in order.

- The $c \rightarrow s$ induced channels like $\Xi_{cc}^{++} \rightarrow \Xi_c^+ l^+ \nu_l$ have a large branching fraction, typically at a few percent level. This is comparable with the branching ratio of semileptonic D decays [52, 53].

TABLE XV: Results for the semi-leptonic decays: the cc sector. The lifetimes of the initial baryons, which are used to derive the branching fractions, can be found in Table IV. Here $l = e/\mu$. Here we have only considered the uncertainties from the heavy quark masses.

Channel	$\Gamma/(10^{-14} \text{ GeV})$	$\mathcal{B}/10^{-3}$	Γ_L/Γ_T
$\Xi_{cc}^{++} \rightarrow \Lambda_c^+ l^+ \nu_l$	0.76 ± 0.37	2.97 ± 1.42	8.5 ± 4.4
$\Xi_{cc}^{++} \rightarrow \Xi_c^+ l^+ \nu_l$	7.72 ± 3.70	30.00 ± 14.40	9.4 ± 5.2
$\Xi_{cc}^+ \rightarrow \Xi_c^0 l^+ \nu_l$	7.72 ± 3.70	5.16 ± 2.47	9.4 ± 5.2
$\Omega_{cc}^+ \rightarrow \Xi_c^0 l^+ \nu_l$	0.61 ± 0.28	1.90 ± 0.87	8.6 ± 4.6
$\Xi_{cc}^{++} \rightarrow \Sigma_c^+ l^+ \nu_l$	0.49 ± 0.29	1.92 ± 1.13	1.1 ± 0.2
$\Xi_{cc}^{++} \rightarrow \Xi_c^{\prime+} l^+ \nu_l$	5.31 ± 3.52	20.70 ± 13.70	1.3 ± 0.2
$\Xi_{cc}^+ \rightarrow \Sigma_c^0 l^+ \nu_l$	0.99 ± 0.58	0.66 ± 0.39	1.1 ± 0.2
$\Xi_{cc}^+ \rightarrow \Xi_c^{\prime0} l^+ \nu_l$	5.31 ± 3.52	3.55 ± 2.36	1.3 ± 0.2
$\Omega_{cc}^+ \rightarrow \Xi_c^{\prime0} l^+ \nu_l$	0.56 ± 0.35	1.76 ± 1.10	1.0 ± 0.2
$\Omega_{cc}^+ \rightarrow \Omega_c^0 l^+ \nu_l$	12.50 ± 8.02	39.00 ± 25.10	1.2 ± 0.2

TABLE XVI: Same as Table XV but for the bb sector.

Channel	$\Gamma/ (10^{-17}\text{GeV})$	$\mathcal{B}/10^{-5}$	Γ_L/Γ_T	Channel	$\Gamma/ (10^{-17}\text{GeV})$	$\mathcal{B}/10^{-5}$	Γ_L/Γ_T
$\Xi_{bb}^- \rightarrow \Lambda_b^0 l^- \bar{\nu}_l$	2.19 ± 1.62	1.23 ± 0.91	7.3 ± 5.3	$\Xi_{bb}^- \rightarrow \Lambda_b^0 \tau^- \bar{\nu}_\tau$	1.03 ± 0.79	0.58 ± 0.44	7.4 ± 5.8
$\Omega_{bb}^- \rightarrow \Xi_b^0 l^- \bar{\nu}_l$	5.34 ± 3.97	6.49 ± 4.83	5.5 ± 4.0	$\Omega_{bb}^- \rightarrow \Xi_b^0 \tau^- \bar{\nu}_\tau$	3.05 ± 2.33	3.71 ± 2.84	5.9 ± 4.7
$\Xi_{bb}^0 \rightarrow \Sigma_b^+ l^- \bar{\nu}_l$	11.70 ± 10.20	6.58 ± 5.73	0.8 ± 0.3	$\Xi_{bb}^0 \rightarrow \Sigma_b^+ \tau^- \bar{\nu}_\tau$	6.42 ± 5.50	3.61 ± 3.09	1.0 ± 0.3
$\Xi_{bb}^- \rightarrow \Sigma_b^0 l^- \bar{\nu}_l$	5.85 ± 5.09	3.29 ± 2.87	0.8 ± 0.3	$\Xi_{bb}^- \rightarrow \Sigma_b^0 \tau^- \bar{\nu}_\tau$	3.21 ± 2.75	1.81 ± 1.55	1.0 ± 0.3
$\Omega_{bb}^- \rightarrow \Xi_b^{\prime0} l^- \bar{\nu}_l$	7.72 ± 6.24	9.39 ± 7.59	0.8 ± 0.3	$\Omega_{bb}^- \rightarrow \Xi_b^{\prime0} \tau^- \bar{\nu}_\tau$	4.20 ± 3.31	5.10 ± 4.02	1.0 ± 0.3

- Compared with Ref. [6], in this work we have considered the contributions from the form factors f_3 and g_3 .

TABLE XVII: Same as Table XV but for the charm decay of bottom-charm baryons.

Channel	$\Gamma/ (10^{-14}\text{GeV})$	$\mathcal{B}/10^{-3}$	Γ_L/Γ_T
$\Xi_{bc}^+ \rightarrow \Lambda_b^0 l^+ \nu_l$	0.82 ± 0.39	3.04 ± 1.46	11.0 ± 6.2
$\Xi_{bc}^+ \rightarrow \Xi_b^0 l^+ \nu_l$	4.37 ± 2.00	16.20 ± 7.40	8.8 ± 5.2
$\Xi_{bc}^0 \rightarrow \Xi_b^- l^+ \nu_l$	4.37 ± 2.00	6.18 ± 2.82	8.8 ± 5.2
$\Omega_{bc}^0 \rightarrow \Xi_b^- l^+ \nu_l$	0.30 ± 0.13	1.01 ± 0.45	8.5 ± 4.8
$\Xi_{bc}^+ \rightarrow \Sigma_b^0 l^+ \nu_l$	0.22 ± 0.15	0.82 ± 0.57	1.5 ± 0.5
$\Xi_{bc}^+ \rightarrow \Xi_b^{\prime0} l^+ \nu_l$	2.52 ± 1.75	9.34 ± 6.50	1.7 ± 0.4
$\Xi_{bc}^0 \rightarrow \Sigma_b^- l^+ \nu_l$	0.44 ± 0.31	0.62 ± 0.44	1.5 ± 0.5
$\Xi_{bc}^0 \rightarrow \Xi_b^{\prime-} l^+ \nu_l$	2.52 ± 1.75	3.56 ± 2.48	1.7 ± 0.4
$\Omega_{bc}^0 \rightarrow \Xi_b^{\prime-} l^+ \nu_l$	0.20 ± 0.13	0.65 ± 0.42	1.4 ± 0.3
$\Omega_{bc}^0 \rightarrow \Omega_b^- l^+ \nu_l$	4.20 ± 2.89	14.10 ± 9.66	1.5 ± 0.3

TABLE XVIII: Same as Table XV but for the bottom decay of bottom-charm baryons.

Channel	$\Gamma/ (10^{-17}\text{GeV})$	$\mathcal{B}/10^{-5}$	Γ_L/Γ_T	Channel	$\Gamma/ (10^{-17}\text{GeV})$	$\mathcal{B}/10^{-5}$	Γ_L/Γ_T
$\Xi_{bc}^0 \rightarrow \Lambda_c^+ l^- \bar{\nu}_l$	8.23 ± 4.78	1.16 ± 0.68	4.8 ± 1.7	$\Xi_{bc}^0 \rightarrow \Lambda_c^+ \tau^- \bar{\nu}_\tau$	6.53 ± 4.03	0.92 ± 0.57	6.1 ± 2.5
$\Omega_{bc}^0 \rightarrow \Xi_c^+ l^- \bar{\nu}_l$	6.99 ± 3.81	2.34 ± 1.27	5.6 ± 2.8	$\Omega_{bc}^0 \rightarrow \Xi_c^+ \tau^- \bar{\nu}_\tau$	4.27 ± 2.49	1.43 ± 0.83	5.8 ± 3.3
$\Xi_{bc}^+ \rightarrow \Sigma_c^{++} l^- \bar{\nu}_l$	17.50 ± 7.78	6.47 ± 2.88	0.5 ± 0.1	$\Xi_{bc}^+ \rightarrow \Sigma_c^{++} \tau^- \bar{\nu}_\tau$	10.50 ± 4.53	3.91 ± 1.68	0.6 ± 0.1
$\Xi_{bc}^0 \rightarrow \Sigma_c^+ l^- \bar{\nu}_l$	8.73 ± 3.89	1.23 ± 0.55	0.5 ± 0.1	$\Xi_{bc}^0 \rightarrow \Sigma_c^+ \tau^- \bar{\nu}_\tau$	5.27 ± 2.26	0.74 ± 0.32	0.6 ± 0.1
$\Omega_{bc}^0 \rightarrow \Xi_c'^+ l^- \bar{\nu}_l$	9.79 ± 4.31	3.28 ± 1.44	0.6 ± 0.1	$\Omega_{bc}^0 \rightarrow \Xi_c'^+ \tau^- \bar{\nu}_\tau$	5.79 ± 2.48	1.94 ± 0.83	0.6 ± 0.1

TABLE XIX: The decay widths (in units of GeV) for the semi-leptonic decays obtained in this work are compared with those from the light-front quark model (LFQM) [6], the heavy quark spin symmetry (HQSS) [64], the nonrelativistic quark model (NRQM) and the MIT bag model (MBM) [62].

Channel	This work	LFQM [6]	HQSS [64]	NRQM [62]	MBM [62]
$\Xi_{cc}^{++} \rightarrow \Lambda_c^+ l^+ \nu_l$	$(7.6 \pm 3.7) \times 10^{-15}$	1.05×10^{-14}	3.20×10^{-15}	1.97×10^{-15}	1.32×10^{-15}
$\Xi_{cc}^{++} \rightarrow \Sigma_c^+ l^+ \nu_l$	$(4.9 \pm 2.9) \times 10^{-15}$	9.60×10^{-15}	5.22×10^{-15}	6.58×10^{-15}	2.63×10^{-15}
$\Xi_{bb}^- \rightarrow \Lambda_b^0 l^- \bar{\nu}_l$	$(2.19 \pm 1.62) \times 10^{-17}$	1.58×10^{-17}	--	--	--
$\Xi_{bb}^- \rightarrow \Sigma_b^0 l^- \bar{\nu}_l$	$(5.85 \pm 5.09) \times 10^{-17}$	3.33×10^{-17}	--	--	--
$\Xi_{bc}^+ \rightarrow \Lambda_b^0 l^+ \nu_l$	$(8.2 \pm 3.9) \times 10^{-15}$	6.85×10^{-15}	--	--	--
$\Xi_{bc}^+ \rightarrow \Sigma_b^0 l^+ \nu_l$	$(2.2 \pm 1.5) \times 10^{-15}$	4.63×10^{-15}	--	--	--
$\Xi_{bc}^0 \rightarrow \Lambda_c^+ l^- \bar{\nu}_l$	$(8.23 \pm 4.78) \times 10^{-17}$	1.84×10^{-17}	--	--	--
$\Xi_{bc}^0 \rightarrow \Sigma_c^+ l^- \bar{\nu}_l$	$(8.73 \pm 3.89) \times 10^{-17}$	4.74×10^{-17}	--	--	--

- In the flavor SU(3) limit, there exist the following relations for the charm quark decay widths:

$$\begin{aligned}
\Gamma(\Xi_{cc}^{++} \rightarrow \Lambda_c^+ l^+ \nu) &= \Gamma(\Omega_{cc}^+ \rightarrow \Xi_c^0 l^+ \nu), \quad \Gamma(\Xi_{cc}^{++} \rightarrow \Xi_c^+ l^+ \nu) = \Gamma(\Xi_{cc}^+ \rightarrow \Xi_c^0 l^+ \nu), \\
\Gamma(\Xi_{cc}^{++} \rightarrow \Sigma_c^+ l^+ \nu) &= \frac{1}{2} \Gamma(\Xi_{cc}^+ \rightarrow \Sigma_c^0 l^+ \nu) = \Gamma(\Omega_{cc}^+ \rightarrow \Xi_c^0 l^+ \nu), \\
\Gamma(\Xi_{cc}^{++} \rightarrow \Xi_c'^+ l^+ \nu) &= \Gamma(\Xi_{cc}^+ \rightarrow \Xi_c^0 l^+ \nu) = \frac{1}{2} \Gamma(\Omega_{cc}^+ \rightarrow \Omega_c^0 l^+ \nu), \\
\Gamma(\Xi_{bc}^+ \rightarrow \Lambda_b^0 l^+ \nu) &= \Gamma(\Omega_{bc}^0 \rightarrow \Xi_b^- l^+ \nu), \quad \Gamma(\Xi_{bc}^+ \rightarrow \Xi_b^0 l^+ \nu) = \Gamma(\Xi_{bc}^0 \rightarrow \Xi_b^- l^+ \nu), \\
\Gamma(\Xi_{bc}^+ \rightarrow \Sigma_b^0 l^+ \nu) &= \frac{1}{2} \Gamma(\Xi_{bc}^0 \rightarrow \Sigma_b^- l^+ \nu) = \Gamma(\Omega_{bc}^0 \rightarrow \Xi_b'^- l^+ \nu), \\
\Gamma(\Xi_{bc}^+ \rightarrow \Xi_b'^0 l^+ \nu) &= \Gamma(\Xi_{bc}^0 \rightarrow \Xi_b'^- l^+ \nu) = \frac{1}{2} \Gamma(\Omega_{bc}^0 \rightarrow \Omega_b^- l^+ \nu).
\end{aligned}$$

For the bottom quark decay, the relations for the decay widths are given as:

$$\begin{aligned}
\Gamma(\Xi_{bb}^- \rightarrow \Lambda_b^0 l^- \bar{\nu}) &= \Gamma(\Omega_{bb}^- \rightarrow \Xi_b^0 l^- \bar{\nu}), \\
\Gamma(\Xi_{bb}^- \rightarrow \Sigma_b^+ l^- \bar{\nu}) &= 2\Gamma(\Xi_{bb}^- \rightarrow \Sigma_b^0 l^- \bar{\nu}) = 2\Gamma(\Omega_{bb}^- \rightarrow \Xi_b^0 l^- \bar{\nu}), \\
\Gamma(\Xi_{bc}^+ \rightarrow \Sigma_c^{++} l^- \bar{\nu}) &= 2\Gamma(\Xi_{bc}^0 \rightarrow \Sigma_c^+ l^- \bar{\nu}) = 2\Gamma(\Omega_{bc}^0 \rightarrow \Xi_c^+ l^- \bar{\nu}).
\end{aligned}$$

Based on the results in Tables XV, XVI, XVII, and XVIII, we find that the SU(3) relations for some channels involving Ω_{bc} and Ω_{bb} are significantly broken.

TABLE XX: The uncertainties of the decay widths of $\Xi_{cc}^{++} \rightarrow \Sigma_c^+ l^+ \nu_l$ caused by those of the form factors in Eq. (44). The central value of the decay width is 4.94×10^{-15} GeV.

f_1	f_2	f_3	g_1	g_2	g_3
9%	14%	0	69%	4%	0

- In Tables XV, XVI, XVII, and XVIII, we have also shown the uncertainties for the phenomenological observables, which come from the uncertainties of $F(0)$'s of the corresponding form factors. The latter uncertainties in turn come from those of the heavy quark masses. In Subsection III A, we have seen that the uncertainty from the heavy quark mass dominates.
- It can be seen from Table XIX that, most results in this work are comparable with those in the literature.

B. Dependence of decay width on the form factors

In this subsection, we will investigate the dependence of decay width on the form factors taking $\Xi_{cc}^{++} \rightarrow \Sigma_c^+ l^+ \nu_l$ as an example. The uncertainties of the decay width caused by those of the form factors in Eq. (44) can be found in Table XX. One can see that these uncertainties are quite different, of which the largest one comes from that of g_1 . In fact, both f_3 and g_3 do not contribute to the decay width. This is because the leptonic part of the amplitude $\bar{\nu} \gamma_\mu (1 - \gamma_5) l$ when contracted with q^μ from the hadronic matrix element vanishes if we neglect the masses of leptons. Finally, it is worth mentioning again that the uncertainty of g_1 mainly comes from that of m_c , as can be seen from Table XIV.

The decay width turns out to be:

$$\Gamma(\Xi_{cc}^{++} \rightarrow \Sigma_c^+ l^+ \nu_l) = (4.94 \pm 3.51) \times 10^{-15} \text{ GeV}. \quad (54)$$

Here we have only considered the uncertainties from $F(0)$'s, and we have also checked that those from m_{pole} and δ can be neglected. Note that here the uncertainties from $F(0)$'s include those from the heavy quark mass m_c , Borel parameter T_1^2 , thresholds s_1^0 and s_2^0 , condensate parameters, pole residues and masses of initial and final baryons. If we only consider the uncertainty from the heavy quark mass m_c for $F(0)$'s, a slightly smaller error is obtained

$$\Gamma(\Xi_{cc}^{++} \rightarrow \Sigma_c^+ l^+ \nu_l) = (4.94 \pm 2.92) \times 10^{-15} \text{ GeV}. \quad (55)$$

It can be seen that, it is a good error estimate for the decay width if we only consider the uncertainties from the heavy quark masses. Thus, in Tables XV, XVI, XVII, and XVIII, only the uncertainties from the heavy quark masses are considered.

V. CONCLUSIONS

Since the observation of doubly charmed baryon Ξ_{cc}^{++} reported by LHCb, many theoretical investigations have been triggered on the hadron spectroscopy and on the weak decays of the doubly heavy baryons, most of which are based on phenomenological models rooted in QCD. In this work, we have presented a first QCD sum rules analysis of the form factors for the doubly heavy baryon decays into singly heavy baryon. We have included the perturbative contribution and condensation contributions up to dimension 5. We have also estimated the partial contributions from the gluon-gluon condensate, and found that these contributions are negligible. These form factors are then used to study the semi-leptonic decays. Future experimental measurements can examine these predictions and test the validity to apply QCDSR to doubly-heavy baryons.

With the advances of new LHCb measurements in future and the under-design experimental facilities, it is anticipated that more theoretical works of analyzing weak decays of doubly-heavy baryons will be conducted. In this direction, we can foresee the following prospects.

- In this study, we have shown that part of the gluon-gluon condensate is small but an analysis with a complete estimate of gluon-gluon condensate is left for future.
- The interpolating currents for baryons are not uniquely determined. An ideal option is to have a largest projection onto the ground state of doubly-heavy baryons and to suppress the contributions from higher resonances and continuum. The dependence on interpolating current and an estimate of the corresponding uncertainties have to be conducted in a systematic way.
- Decay form factors calculated in this work are induced by heavy to light transitions, and the heavy to heavy transition will be studied in future. Another plausible framework is the non-relativistic QCD.
- We have investigated the form factors defined by vector and axial-vector currents, while the tensor form factor are necessary to study the flavor-changing neutral current processes in bottom quark decays, like the radiative and the dilepton decay modes.
- We have focused on the final baryons with spin-1/2, while the $1/2 \rightarrow 3/2$ transition needs an independent analysis.
- Our calculation of the form factors is conducted at the leading order in the expansion of strong coupling constant. However, to achieve a more precise result, it is still necessary to perform the calculation of higher order radiative corrections in future works.
- The ordinary QCD sum rules makes use of small- x OPE. In heavy to light transition, there exists a large momentum transfer and it would be advantageous to adopt the light-cone

OPE. Recently, the authors of Ref. [65] conducted the light-cone QCDSR study, and similar results are obtained.

Acknowledgements

The authors are grateful to Hai-Yang Cheng, Pietro Colangelo, Jürgen Körner, Run-Hui Li, Yu-Ming Wang, Zhi-Gang Wang, Fan-Rong Xu, Mao-Zhi Yang, Fu-Sheng Yu for useful discussions. This work is supported in part by National Natural Science Foundation of China under Grants No.11575110, 11735010,11911530088, Natural Science Foundation of Shanghai under Grants No. 15DZ2272100, and by Key Laboratory for Particle Physics, Astrophysics and Cosmology, Ministry of Education.

-
- [1] R. Aaij *et al.* [LHCb Collaboration], Phys. Rev. Lett. **119**, no. 11, 112001 (2017) doi:10.1103/PhysRevLett.119.112001 [arXiv:1707.01621 [hep-ex]].
 - [2] R. Aaij *et al.* [LHCb Collaboration], Phys. Rev. Lett. **121**, no. 5, 052002 (2018) doi:10.1103/PhysRevLett.121.052002 [arXiv:1806.02744 [hep-ex]].
 - [3] R. Aaij *et al.* [LHCb Collaboration], Phys. Rev. Lett. **121**, no. 16, 162002 (2018) doi:10.1103/PhysRevLett.121.162002 [arXiv:1807.01919 [hep-ex]].
 - [4] M. T. Traill [LHCb Collaboration], PoS Hadron **2017**, 067 (2018). doi:10.22323/1.310.0067
 - [5] A. Cerri *et al.*, arXiv:1812.07638 [hep-ph].
 - [6] W. Wang, F. S. Yu and Z. X. Zhao, Eur. Phys. J. C **77**, no. 11, 781 (2017) doi:10.1140/epjc/s10052-017-5360-1 [arXiv:1707.02834 [hep-ph]].
 - [7] L. Meng, N. Li and S. l. Zhu, Eur. Phys. J. A **54**, no. 9, 143 (2018) doi:10.1140/epja/i2018-12578-2 [arXiv:1707.03598 [hep-ph]].
 - [8] W. Wang, Z. P. Xing and J. Xu, Eur. Phys. J. C **77**, no. 11, 800 (2017) doi:10.1140/epjc/s10052-017-5363-y [arXiv:1707.06570 [hep-ph]].
 - [9] T. Gutsche, M. A. Ivanov, J. G. Krner and V. E. Lyubovitskij, Phys. Rev. D **96**, no. 5, 054013 (2017) doi:10.1103/PhysRevD.96.054013 [arXiv:1708.00703 [hep-ph]].
 - [10] H. S. Li, L. Meng, Z. W. Liu and S. L. Zhu, Phys. Lett. B **777**, 169 (2018) doi:10.1016/j.physletb.2017.12.031 [arXiv:1708.03620 [hep-ph]].
 - [11] Z. H. Guo, Phys. Rev. D **96**, no. 7, 074004 (2017) doi:10.1103/PhysRevD.96.074004 [arXiv:1708.04145 [hep-ph]].
 - [12] Q. F. L, K. L. Wang, L. Y. Xiao and X. H. Zhong, Phys. Rev. D **96**, no. 11, 114006 (2017) doi:10.1103/PhysRevD.96.114006 [arXiv:1708.04468 [hep-ph]].
 - [13] L. Y. Xiao, K. L. Wang, Q. f. Lu, X. H. Zhong and S. L. Zhu, Phys. Rev. D **96**, no. 9, 094005 (2017) doi:10.1103/PhysRevD.96.094005 [arXiv:1708.04384 [hep-ph]].
 - [14] N. Sharma and R. Dhir, Phys. Rev. D **96**, no. 11, 113006 (2017) doi:10.1103/PhysRevD.96.113006 [arXiv:1709.08217 [hep-ph]].

- [15] Y. L. Ma and M. Harada, *J. Phys. G* **45**, no. 7, 075006 (2018) doi:10.1088/1361-6471/aac86e [arXiv:1709.09746 [hep-ph]].
- [16] F. S. Yu, H. Y. Jiang, R. H. Li, C. D. L, W. Wang and Z. X. Zhao, *Chin. Phys. C* **42**, no. 5, 051001 (2018) doi:10.1088/1674-1137/42/5/051001 [arXiv:1703.09086 [hep-ph]].
- [17] L. Meng, H. S. Li, Z. W. Liu and S. L. Zhu, *Eur. Phys. J. C* **77**, no. 12, 869 (2017) doi:10.1140/epjc/s10052-017-5447-8 [arXiv:1710.08283 [hep-ph]].
- [18] X. H. Hu, Y. L. Shen, W. Wang and Z. X. Zhao, *Chin. Phys. C* **42**, no. 12, 123102 (2018) doi:10.1088/1674-1137/42/12/123102 [arXiv:1711.10289 [hep-ph]].
- [19] E. L. Cui, H. X. Chen, W. Chen, X. Liu and S. L. Zhu, *Phys. Rev. D* **97**, no. 3, 034018 (2018) doi:10.1103/PhysRevD.97.034018 [arXiv:1712.03615 [hep-ph]].
- [20] Y. J. Shi, W. Wang, Y. Xing and J. Xu, *Eur. Phys. J. C* **78**, no. 1, 56 (2018) doi:10.1140/epjc/s10052-018-5532-7 [arXiv:1712.03830 [hep-ph]].
- [21] L. Y. Xiao, Q. F. L and S. L. Zhu, *Phys. Rev. D* **97**, no. 7, 074005 (2018) doi:10.1103/PhysRevD.97.074005 [arXiv:1712.07295 [hep-ph]].
- [22] X. Yao and B. Mller, *Phys. Rev. D* **97**, no. 7, 074003 (2018) doi:10.1103/PhysRevD.97.074003 [arXiv:1801.02652 [hep-ph]].
- [23] D. L. Yao, *Phys. Rev. D* **97**, no. 3, 034012 (2018) doi:10.1103/PhysRevD.97.034012 [arXiv:1801.09462 [hep-ph]].
- [24] U. zdem, *J. Phys. G* **46**, no. 3, 035003 (2019) doi:10.1088/1361-6471/aafffc [arXiv:1804.10921 [hep-ph]].
- [25] A. Ali, A. Y. Parkhomenko, Q. Qin and W. Wang, *Phys. Lett. B* **782**, 412 (2018) doi:10.1016/j.physletb.2018.05.055 [arXiv:1805.02535 [hep-ph]].
- [26] J. M. Dias, V. R. Debastiani, J.-J. Xie and E. Oset, *Phys. Rev. D* **98**, no. 9, 094017 (2018) doi:10.1103/PhysRevD.98.094017 [arXiv:1805.03286 [hep-ph]].
- [27] R. H. Li and C. D. Lu, arXiv:1805.09064 [hep-ph].
- [28] Z. X. Zhao, *Eur. Phys. J. C* **78**, no. 9, 756 (2018) doi:10.1140/epjc/s10052-018-6213-2 [arXiv:1805.10878 [hep-ph]].
- [29] Y. Xing and R. Zhu, *Phys. Rev. D* **98**, no. 5, 053005 (2018) doi:10.1103/PhysRevD.98.053005 [arXiv:1806.01659 [hep-ph]].
- [30] R. Zhu, X. L. Han, Y. Ma and Z. J. Xiao, *Eur. Phys. J. C* **78**, 740 (2018) doi:10.1140/epjc/s10052-018-6214-1 [arXiv:1806.06388 [hep-ph]].
- [31] A. Ali, Q. Qin and W. Wang, *Phys. Lett. B* **785**, 605 (2018) doi:10.1016/j.physletb.2018.09.018 [arXiv:1806.09288 [hep-ph]].
- [32] M. Z. Liu, Y. Xiao and L. S. Geng, *Phys. Rev. D* **98**, no. 1, 014040 (2018) doi:10.1103/PhysRevD.98.014040 [arXiv:1807.00912 [hep-ph]].
- [33] Z. P. Xing and Z. X. Zhao, *Phys. Rev. D* **98**, no. 5, 056002 (2018) doi:10.1103/PhysRevD.98.056002 [arXiv:1807.03101 [hep-ph]].
- [34] R. Aaij *et al.* [LHCb Collaboration], arXiv:1808.08865.
- [35] W. Wang and R. Zhu, arXiv:1808.10830 [hep-ph].
- [36] R. Dhir and N. Sharma, *Eur. Phys. J. C* **78**, no. 9, 743 (2018). doi:10.1140/epjc/s10052-018-6220-3
- [37] A. V. Berezhnoy, A. K. Likhoded and A. V. Luchinsky, *Phys. Rev. D* **98**, no. 11, 113004 (2018) doi:10.1103/PhysRevD.98.113004 [arXiv:1809.10058 [hep-ph]].
- [38] L. J. Jiang, B. He and R. H. Li, *Eur. Phys. J. C* **78**, no. 11, 961 (2018) doi:10.1140/epjc/s10052-018-6445-1 [arXiv:1810.00541 [hep-ph]].

- [39] Q. A. Zhang, Eur. Phys. J. C **78**, no. 12, 1024 (2018) doi:10.1140/epjc/s10052-018-6481-x [arXiv:1811.02199 [hep-ph]].
- [40] G. Li, X. F. Wang and Y. Xing, Eur. Phys. J. C **79**, no. 3, 210 (2019) doi:10.1140/epjc/s10052-019-6729-0 [arXiv:1811.03849 [hep-ph]].
- [41] L. Meng and S. L. Zhu, Phys. Rev. D **100**, no. 1, 014006 (2019) doi:10.1103/PhysRevD.100.014006 [arXiv:1811.07320 [hep-ph]].
- [42] T. Gutsche, M. A. Ivanov, J. G. Krner, V. E. Lyubovitskij and Z. Tyulemissov, Phys. Rev. D **99**, no. 5, 056013 (2019) doi:10.1103/PhysRevD.99.056013 [arXiv:1812.09212 [hep-ph]].
- [43] A. I. Onishchenko, hep-ph/0006271.
- [44] A. I. Onishchenko, hep-ph/0006295.
- [45] V. V. Kiselev and A. K. Likhoded, Phys. Usp. **45**, 455 (2002) [Usp. Fiz. Nauk **172**, 497 (2002)] doi:10.1070/PU2002v045n05ABEH000958 [hep-ph/0103169].
- [46] J. R. Zhang and M. Q. Huang, Phys. Rev. D **78**, 094007 (2008) doi:10.1103/PhysRevD.78.094007 [arXiv:0810.5396 [hep-ph]].
- [47] Z. G. Wang, Eur. Phys. J. A **45**, 267 (2010) doi:10.1140/epja/i2010-11004-3 [arXiv:1001.4693 [hep-ph]].
- [48] Z. G. Wang, Eur. Phys. J. C **68**, 459 (2010) doi:10.1140/epjc/s10052-010-1357-8 [arXiv:1002.2471 [hep-ph]].
- [49] Z. G. Wang, Eur. Phys. J. A **47**, 81 (2011) doi:10.1140/epja/i2011-11081-8 [arXiv:1003.2838 [hep-ph]].
- [50] B. L. Ioffe, Prog. Part. Nucl. Phys. **56**, 232 (2006) doi:10.1016/j.ppnp.2005.05.001 [hep-ph/0502148].
- [51] P. Colangelo and A. Khodjamirian, In *Shifman, M. (ed.): At the frontier of particle physics, vol. 3* 1495-1576 doi:10.1142/9789812810458_0033 [hep-ph/0010175].
- [52] C. Patrignani *et al.* [Particle Data Group], Chin. Phys. C **40**, no. 10, 100001 (2016). doi:10.1088/1674-1137/40/10/100001
- [53] M. Tanabashi *et al.* [Particle Data Group], Phys. Rev. D **98**, no. 3, 030001 (2018). doi:10.1103/PhysRevD.98.030001
- [54] Z. G. Wang, Eur. Phys. J. C **68**, 479 (2010) doi:10.1140/epjc/s10052-010-1365-8 [arXiv:1001.1652 [hep-ph]].
- [55] Z. G. Wang, Phys. Lett. B **685**, 59 (2010) doi:10.1016/j.physletb.2010.01.039 [arXiv:0912.1648 [hep-ph]].
- [56] Z. S. Brown, W. Detmold, S. Meinel and K. Orginos, Phys. Rev. D **90**, no. 9, 094507 (2014) doi:10.1103/PhysRevD.90.094507 [arXiv:1409.0497 [hep-lat]].
- [57] W. Roberts and M. Pervin, Int. J. Mod. Phys. A **23**, 2817 (2008) doi:10.1142/S0217751X08041219 [arXiv:0711.2492 [nucl-th]].
- [58] M. Karliner and J. L. Rosner, Phys. Rev. D **90**, no. 9, 094007 (2014) doi:10.1103/PhysRevD.90.094007 [arXiv:1408.5877 [hep-ph]].
- [59] H. Y. Cheng and Y. L. Shi, Phys. Rev. D **98**, no. 11, 113005 (2018) doi:10.1103/PhysRevD.98.113005 [arXiv:1809.08102 [hep-ph]].
- [60] Z. G. Wang, Eur. Phys. J. A **49**, 131 (2013) doi:10.1140/epja/i2013-13131-7 [arXiv:1203.6252 [hep-ph]].
- [61] P. Ball, V. M. Braun and H. G. Dosch, Phys. Rev. D **44**, 3567 (1991). doi:10.1103/PhysRevD.44.3567
- [62] R. Perez-Marcial, R. Huerta, A. Garcia and M. Avila-Aoki, Phys. Rev. D **40**, 2955 (1989) Erratum: [Phys. Rev. D **44**, 2203 (1991)]. doi:10.1103/PhysRevD.44.2203, 10.1103/PhysRevD.40.2955
- [63] L. J. Carson, R. J. Oakes and C. R. Willcox, Phys. Rev. D **33**, 1356 (1986). doi:10.1103/PhysRevD.33.1356

- [64] C. Albertus, E. Hernandez and J. Nieves, PoS QNP **2012**, 073 (2012) doi:10.22323/1.157.0073 [arXiv:1206.5612 [hep-ph]].
- [65] Y. J. Shi, Y. Xing and Z. X. Zhao, Eur. Phys. J. C **79**, no. 6, 501 (2019) doi:10.1140/epjc/s10052-019-7014-y [arXiv:1903.03921 [hep-ph]].